SEVENTH FRAMEWORK PROGRAMME

FP7-SPACE-2009-1

MONARCH - A

MONitoring and Assessing Regional Climate change in High latitudes and the Arctic

Working paper:

Deliverable No. 1.2.2: Water level variations over the large Arctic lakes from satellite altimeters

Deliverable No. 1.2.3: Water level variations and river discharge of the large Arctic river from satellite altimeters and in situ data related to input into Arctic ocean

A.V. Kouraev, E.A. Zakharova, N.M. Mognard

Version: March 2011

Grant agreement no.: 242446
Project Coordinator: Johnny Johannessen
Project home page: http://monarch-a.nersc.no

Laboratoire d'Etudes en Géophysique et Océanographie Spatiales
UMR5566 (CNES-CNRS-IRD-UPS)

Groupe de Recherche de Géodésie Spatiale
Observatoire Midi-Pyrénées

1. Introduction

The aim of this working paper is to provide a description for the a) water level variations over the large Arctic lakes from satellite altimeters and b) water level variations and river discharge of the large Arctic river from satellite altimeters and in situ data related to input into Arctic ocean. These data are a contribution to the Work Package 1.2 "The decadal dynamics of high-latitude lakes and their consequences for GHGs and climate.

Arctic rivers and lakes are an integral part of the global climate system, sensitive to its regional and global variations. and therefore a strong indicator of climate change. Global warming is expected to be the most significant with strong feedback on global climate in the arctic regions [IPCC, 2001]. Climatic change will lead to potential increase in fresh water release into the Arctic Ocean, which in turn will affect thermohaline circulation, as well as ice and North Atlantic Deep Water (NADW) formation [Rahmstorf, 1995 ; Broecker, 1997]. Peterson et al. (2002) have shown using in situ river monitoring data that the average annual discharge of fresh water from the largest Eurasian rivers to the Arctic Ocean has already increased by 7% from 1936 to 1999.

In situ measurements of important environmental parameters such as water level (for lakes and rivers) and river discharge are rather sparse in the remote Arctic

environments. Besides this, a general decline in the arctic hydrologic monitoring network has begun in the mid 1980s [Shiklomanov et al., 2002]. These conditions make microwave satellite sensors measurements an essential complement to in situ observations, and in some cases, to serve as virtual gauging stations. Satellite radar altimetry could provide valuable information on water level variations of lakes, rivers, wetlands and floodplains with the precision of several tens of centimetres [Birkett, 1995, 1998; Mercier, 2001; de Oliveira Campos et al., 2001; Bjerklie et al., 2003; Maheu et al., 2003]. Here we present the results of altimetric measurements of water level over the Arctic lakes and rivers, discuss several issues affecting the accuracy of these data. We assess the potential of monitoring water level of wetlands, as well as reconstructing river discharge from satellite observations of water level (on the example of the Ob' river). We also present the in situ data on river level and discharge available through ArcticRIMS web site.

2. Source data

2.1. Satellite altimetry.

2.1.1. Principles of satellite radar altimetry and various satellite missions.

A satellite radar altimeter performs vertical range measurements between the satellite and the reflecting water surface. The difference between the satellite altitude above a reference surface (either a conventional ellipsoid or a model geoid surface) determined through precise orbit computation, and the distance from the satellite to the water provides a measurement of the water level above the reference surface

(altimeter range). Placed onto a repeat orbit, the satellite altimeter overflies a given region at regular time intervals (called the orbital cycle).

Although the primary mission of satellite altimetry is the study of sea surface topography over the open ocean, this technique has been successfully applied to continental surfaces to monitor water level of inland seas such as Caspian and Aral seas [Cazenave et al., 1999; Aladin et al., 2005, Crétaux et al., 2005], large lakes [Ponchaut and Cazenave, 1998; Mercier et al., 2002, Crétaux and Birkett, 2006], as well as large rivers, wetlands and floodplains [Birkett, 1998; de Oliveira Campos et al., 2001, Maheu et al., 2003, Papa et al., 2006, Prigent et al., 2007]. Satellite altimetry has been used not only to derive river level, but also to reconstruct river discharge from the Ob' and Amazon rivers [Kouraev et al., 2004, Zakharova et al., 2006].

Several radar altimetry missions provide data on water level. The earliest data are available from the TOPEX/Poseidon (T/P) satellite, operating since 1992. In August 2002, T/P was manoeuvred onto a new orbit, flying halfway between its previous tracks. The T/P mission ended in October 2005. T/P has been followed by Jason-1, orbiting on the same ground track since February 2002. In June 2008 a new satellite, OSTM/Jason-2, has been launched on the same orbit. Both Jason-1 and OSTM/Jason-2 had one-minute shift (55 seconds, exactly). On mid-February, 2009, Jason-1 assumed a new orbit midway between its original ground tracks but with a time lag of approximately 5 days with OSTM/Jason-2. This new tandem configuration better suits for real-time applications. The former T/P ground tracks are now overflown by OSTM/Jason-2 [http://www.aviso.oceanobs.com/en/missions/current-missions/jason-1/index.html].

The T/P and Jason-1,-2 data are complemented by observations from radar altimeters onboard Geosat Follow-On (GFO) (January 2000 - November 2008) and ENVISAT (since November 2002) satellites. S-band module of the ENVISAT RA-2 radar altimeter has been lost since 2008/01/18. To ensure an additional 3 years lifespan, the ENVISAT satellite has been moved to a new lower orbit on October 22, 2010. T/P and Jason-1,-2 satellites have 10-days repeat orbit, GFO - 17 days, ENVISAT - 35 days. From 02 November 2010, both the ground track and, consequently, the repeat cycle have been changed for ENVISAT: 30 days with 431 orbits per cycle instead of 35 days-501 orbits per cycle

All altimeters have two main nadir-looking instruments – a dual-frequency (single-frequency for GFO) radar altimeter operating in Ku (13.6 GHz), C (5 GHz) or S (2 GHz) bands, and a passive microwave radiometer operating at two or three frequencies used to obtain environmental corrections.

2.1.2. Environmental corrections and geographic selection

In order to obtain good estimates of water levels over lakes and rivers, various environmental and geophysical corrections of the altimeter range measurements relevant to the water body should be applied. The corrections applied usually include ionospheric, dry tropospheric, solid Earth tide corrections and correction for the satellite's centre of gravity. Could be neglected, on the other hand, corrections specific to open ocean environments such as ocean and pole tides, ocean tide loading, inverted barometer effect and sea state bias. The wet tropospheric correction,

normally derived from the onboard radiometers over oceans, is not available over land. The radiometers have a large footprint (up to 43.4 km in diameter for the 18 GHz channel), and when the satellite flies over rivers or lakes, the TMR footprint almost always includes surrounding lands, which contaminates the measurements and makes atmospheric water vapour measurement unreliable. However, over land, the wet tropospheric correction can be modelled using meteorological operational analyses using air temperature and specific humidity fields, such as from NCEP (National Centers for Environmental Predictions) meteorological fields. The water level is usually referred to the geoid surface.

The theoretical footprint of the altimeter data over the open ocean is about 10-12 km (for Ku band, depending on surface roughness). However, for smooth surfaces, that provide a quasi-specular return signal, the main part of the backscatter signal comes from a much smaller area. Among these surfaces are a) ice cover, where largest part of signal comes from the area with a diameter of 1-2 km [Legresy and Remy, 1997] and b) calm water, which is often observed for small water bodies, flooded areas etc.

A mountainous topography may lead the altimeter to lock off completely, requiring some time to lock on again, even over water and for narrow rivers, the instrument may deliver no reliable measurement at all. In other cases, the instrument could remain locked on water while the satellite is well ahead of the water body, since the reflected signal on water has more power than the reflected signal on land. This may cause a geometric error that could reach several meters for some regions.

In order to minimise potential contamination of the altimetric signal by land reflections, and at the same time to retain a sufficiently large number of altimeter measurements on water, a geographical selection of the data is necessary. This could be done using high-resolution reference satellite imagery (such as GeoCover™ Landsat Thematic Mapper orthorectified mosaics) to select the most appropriate intersections of water bodies and satellite tracks. Another solution could be the use of the data with the highest possible along track ground resolution, such as 10 Hz data for T/P and 18 Hz for ENVISAT (distance between adjacent altimetric observations is about 600 and 400 m, correspondingly).

2.1.3. Influence of ice cover on water level measurements

For arctic rivers and lakes presence of ice cover could affect the accuracy of radar altimetry measurements of water level. Estimates of range between satellite and the echoing surface are obtained using procedures known as altimeter waveform retracking. Retracking retrieves the point of the radar echo that correspond to the effective satellite-to-ground range. As the primary goal of most altimeters is the study of ocean topography, most of the retracking algorithms used are suited to the open ocean conditions. For example, T/P, Jason-1, and GFO all have only one on-board retracker that is adapted to the ocean surface. However, for arctic lakes and rivers stable ice cover present every year for several months, and this significantly affects the shape of the returning radar waveform and could result in erroneous range estimates in the winter.

In order to assess the degree in which ice presence affects altimeter range measures and estimate uncertainties, data from ENVISAT altimeter has been used for the Aral sea (Kouraev et al., 2009; see Annex 1). For this satellite four different retracking algorithms (one - Ocean - for ocean conditions and three - Ice1, Ice2 and Sea Ice - for ice) are used to process raw RA-2 radar altimeter data. Presence of the four simultaneous range values from these retrackers for each 18 Hz RA-2 measure gives a possibility to precisely quantify the difference between various retrackers.

When the Aral sea is ice-covered, Sea Ice and Ice 2 values are close to each other. Ice1 provides sea level position 15-20 cm higher, what is also related to its retracking algorithm. However, Ocean retracker constantly shows much higher values than any ice-adapted retracker, with differences coming up to 40-45 cm. This is related to differences of waveform shapes between ocean and other types of surface. For example, for the ice-covered Ob' river in Siberia, comparison of T/P water level and in situ observations at closest hydrological point at Salekhard showed that for complex terrains with influence of land and river ice T/P overestimated the range (and thus underestimated the level) for up to 2-3 m [Kouraev et al., 2004].

Thus, for ENVISAT, it is obviously better to use other retrackers than Ocean when ice cover is present. While for the Aral sea we have not been able to estimate the absolute difference for each altimetric satellite, it looks reasonable to adjust sea level measures from T/P, Jason-1 and GFO (that all use Ocean retracker) 40-45 cm lower.

2.1.4. Sources of altimetric data

The initial GDR altimetry data have been obtained from the Centre for Topographic studies of the Oceans and Hydrosphere (CTOH) at the LEGOS laboratory (http://www.legos.obs-mip.fr/en/observations/ctoh/).

Processed time series of the lake and river level has been obtained from the Hydroweb web site [http://www.legos.obs-mip.fr/en/equipes/gohs/resultats/i_hydroweb]. This altimetric water level data base at LEGOS (Laboratory of Space Geophysics and Oceanography), Toulouse, France, contains time series over water levels of large rivers, lakes and wetlands around the world. These time series are mainly based on altimetry data from T/P for rivers, but ERS-1 & 2, Envisat, Jason-1 and GFO data are also used for lakes. At present, water level time series for about 100 lakes and 250 sites (called virtual stations) on large rivers are available. The altimeter range measurements used for lakes consist of 1Hz data. For large water bodies the satellite data should be averaged long distances and it is necessary to correct for the slope of the geoid (or, equivalently, the mean lake level). Because the reference geoid provided with the altimetry measurements (e.g., EGM96 for T/P data) may not be accurate enough, a mean lake level is computed, averaging over time the altimetry measurements themselves. The water levels are further referred to this ‘mean lake level’. Each satellite data are processed independently and potential radar instrument biases between different satellites are removed using T/P data as reference. Then lake levels from the different satellites are merged on a monthly basis.

2.2. In situ data on river level and discharge (ArcticRIMS)

Satellite radar altimetry is a useful complement to the other sources of information, often providing the data for the regions not covered by the standard network of hydrometeorological stations. However for the observations of river level and river discharge in situ data, when available, still are the reference. For the arctic rivers in this respect a very good source of information is presented by the ArcticRIMS (A Regional, Integrated Hydrological Monitoring Systemfor the Pan-Arctic Land Mass) web site [http://rims.unh.edu/index.shtml] (Figure 1).

Figure 1. ArcticRIMS web site screenshot.

The subject of this web site is the near-real time monitoring of pan- Arctic water budgets and river discharge to the Arctic Ocean though providing a spatially and temporally-harmonized data set for pan-Arctic hydrology and meteorology. Among various data presented, the most relevant for the Monarch-A project are daily and monthly observations of water level and discharge for main rivers flowing to the Arctic Ocean, that are freely available online.

3. Water level of large Arctic lakes, reservoirs and wetlands

3.1. Arctic lakes

Temporal variability of water level of large Arctic and boreal lakes from satellite radar altimetry is presented in the directory Lake Level. These are the data from the Hydroweb web site (see section 2.1.4). File format - ASCII, with three columns - time or date (fraction of the year), water level or height (m, above GGM02C geoid) and standard deviation of level (m). Data for each lake or reservoir are stored in the file with the corresponding name.

Water level time series for these lakes and reservoirs are presented on figures 3-6. The biggest seasonal and interannual amplitude is characteristic for reservoirs. It should be noted, that for many lakes water level is now controlled by the hydroelectric power plants or dams. Thus for Il'men' Lake water level is regulated by the Volkhov hydroelectric plant, for Lake Vaettern - by a controlled canal, for Onega lake - by the Verkhesvir'skaya power plant; Lake Saint-Jean has dams on outflowing Alma and Peribonka rivers etc. Thus water level changes on these lakes reflect not that much natural variability of the water budget, as the human response to this variability in the context of water management.

a)

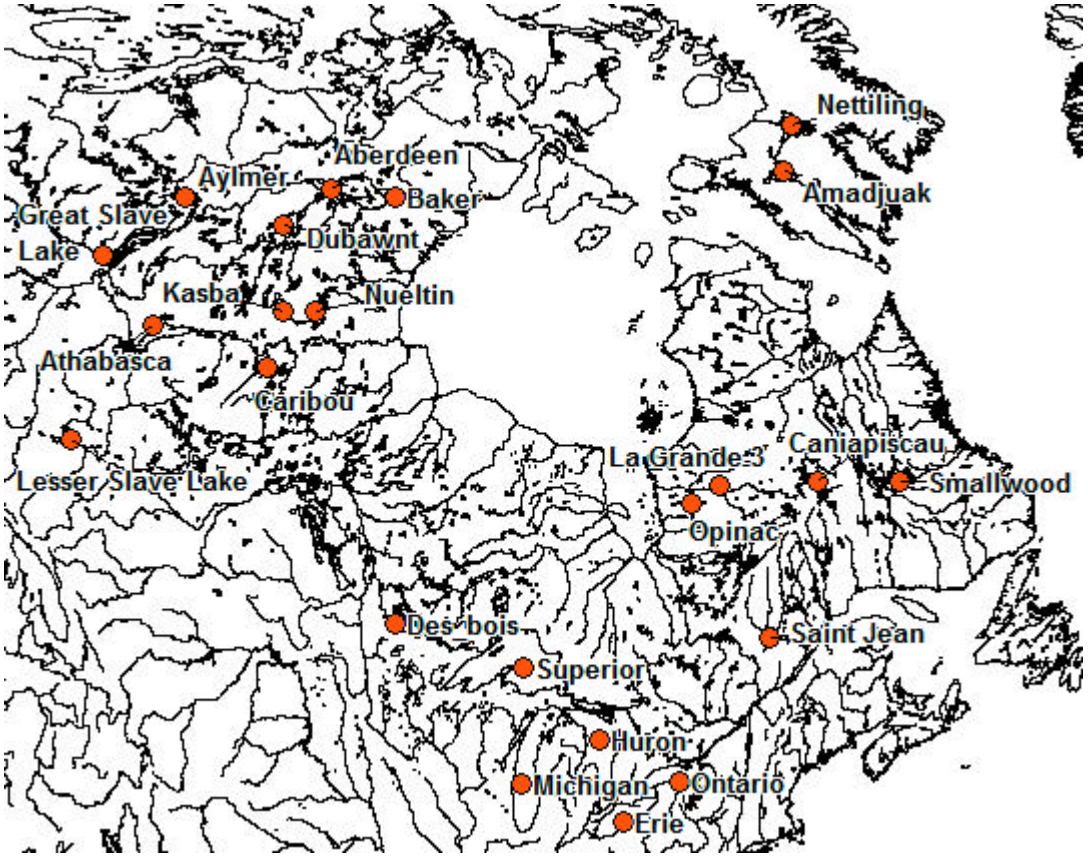

b)

Figure 2. Lakes and reservoirs in Eurasia (a) and Northern America (b) for which time series of altimetric water level are provided.

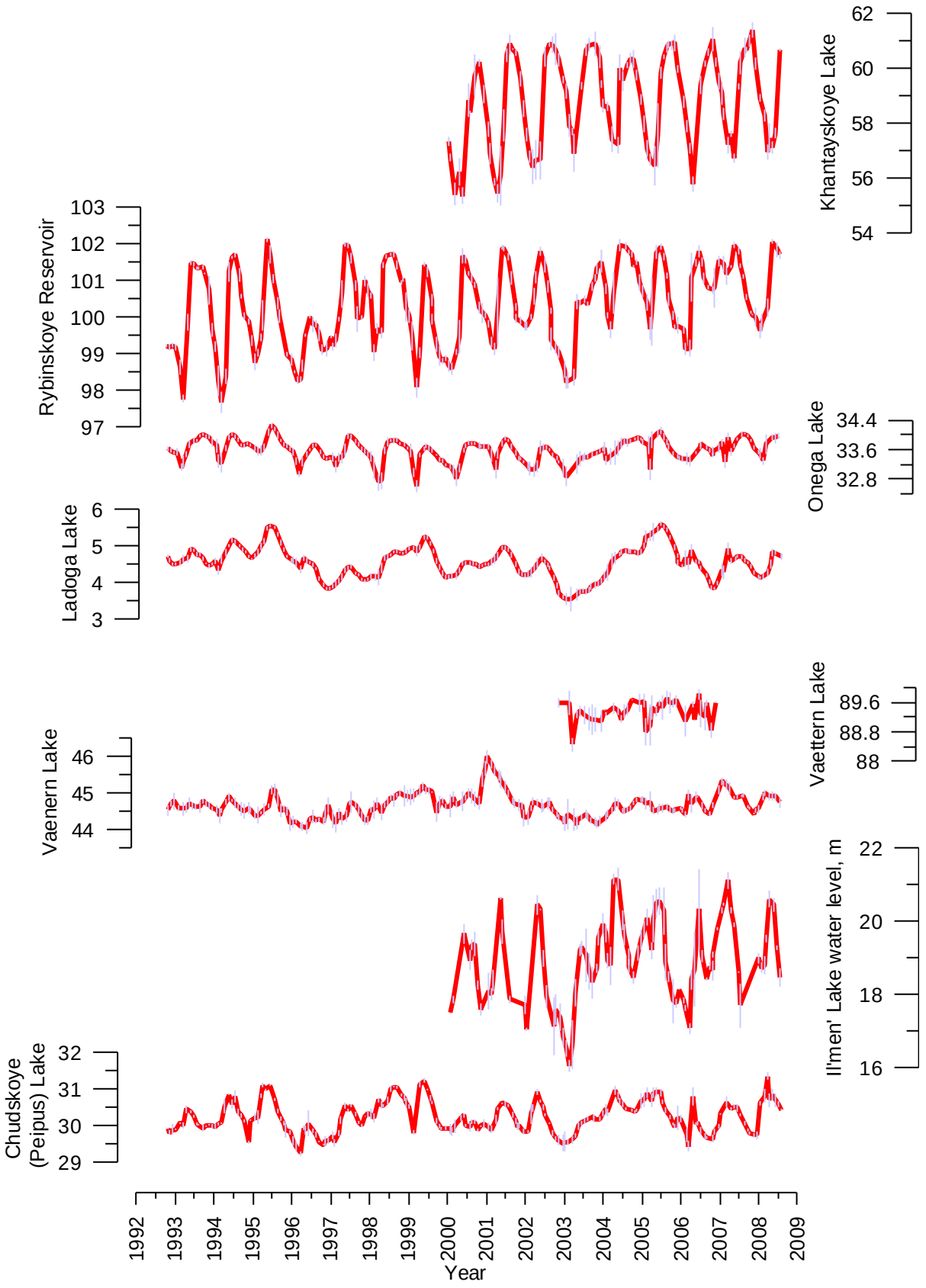

Figure 3. Water level variability (m, above geoid) of the Eurasian lakes and reservoirs. Red line - mean values, light blue bars -standard deviation. All Y axis on this figure have the same vertical scale

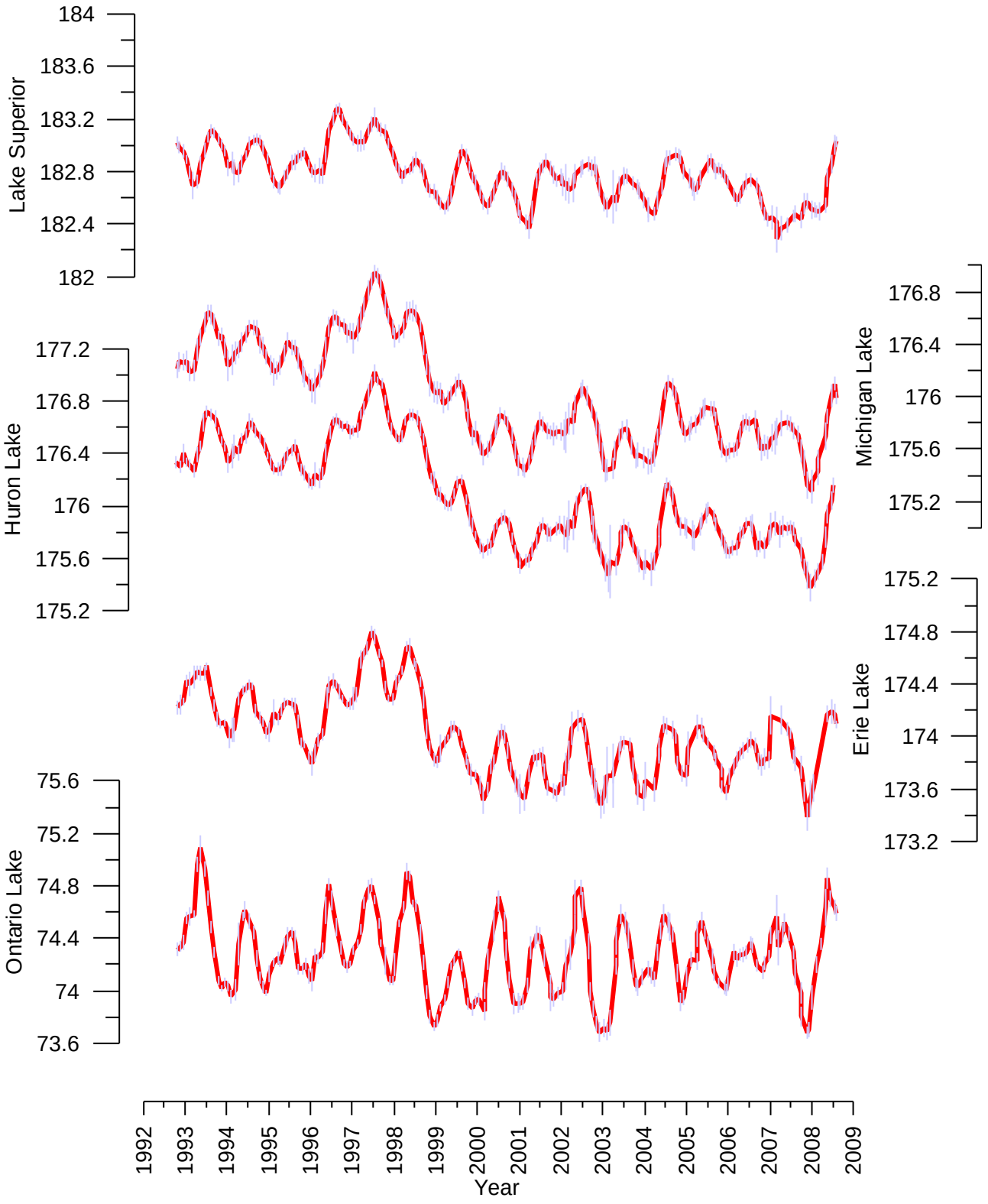

Figure 4. Same as figure 3, but for the Great Lakes.

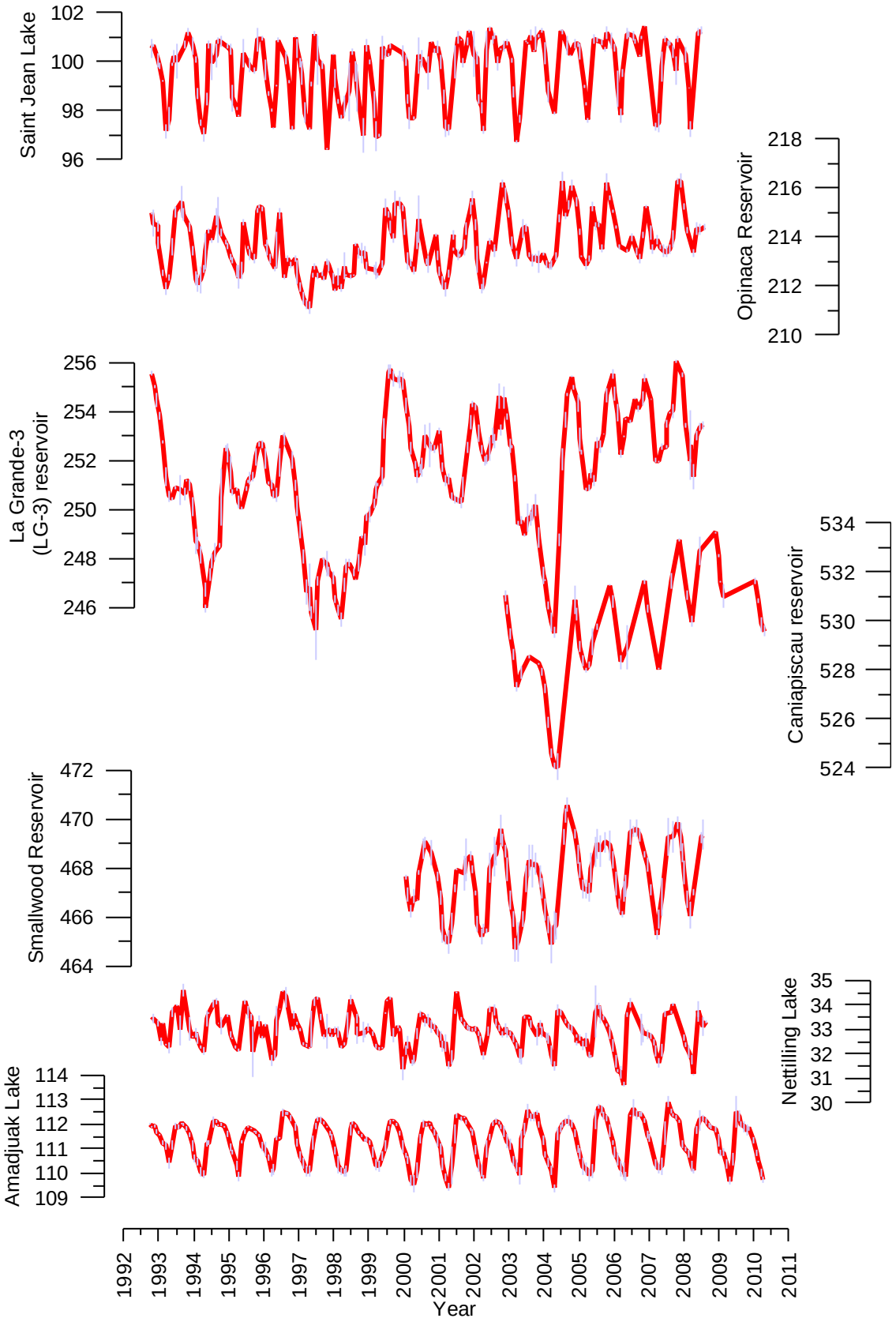

Figure 5. Same as figure 3, but for the North-Eastern Canada.

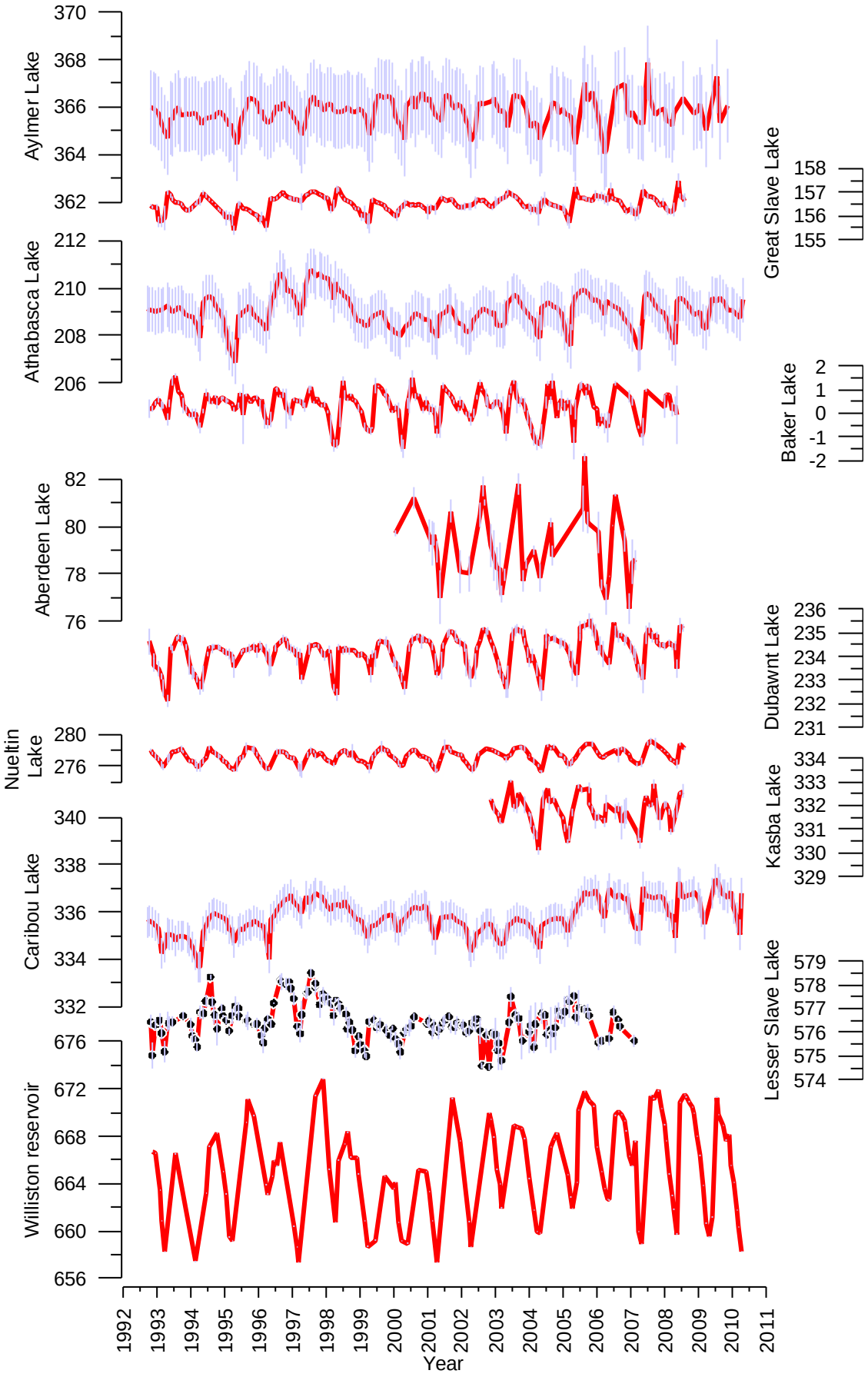

Figure 6. Same as figure 3, but for the North-Western Canada. All Y axis on this figure have the same vertical scale (except for Williston reservoir, reduced two times)

3.2. Water level variability over mall lakes, mires and wetlands

Another potentially interesting application of radar altimetry is the monitoring of water level changes of small lakes, bogs and wetlands. For areas with flat relief, such as the Western Siberia, topography affects the hydrographical network, creating a multitude of interconnected natural objects - large and small rivers and streams, extensive floodplains, lakes, mires etc. The presence of large flooded areas, lakes and mires in Western Siberia results in a rate of evaporation higher than for any other large boreal watershed. One of these wetland types - mires – is crucial in the global carbon cycle. Mires sequester carbon through photosynthesis and accumulation in peat deposits, acting as a terrestrial sink of atmospheric carbon. But, in the permafrost regions of Western Siberia, mires are a source of methane emission to the atmosphere.

For regions with relatively homogeneous surface type, radar altimetry can provide estimations of water level changes. An example of this application is shown on Figures 7-8. Two regions - Nadym and Surgut swamps have been identified and water level variability for various water bodies has been analysed using ENVISAT 18 Hz data. The highest water variability (from 1 to 1.5 meters) is typical for lakes, while for flat mires and drained lakes (khasyreys) it is much smaller (50-70 cm). We observe that wetlands have the regulating (dampening) effect on water level variability.

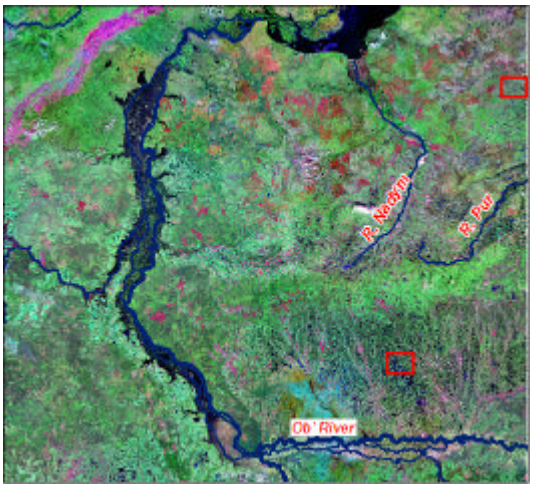

a)

b)

c)

Figure 7. a) Location of the two study regions and typical landscape photos for Nadym swaps in the Northern part of the Western Siberia (b) and Surgut swaps in the Middle Ob' (c).

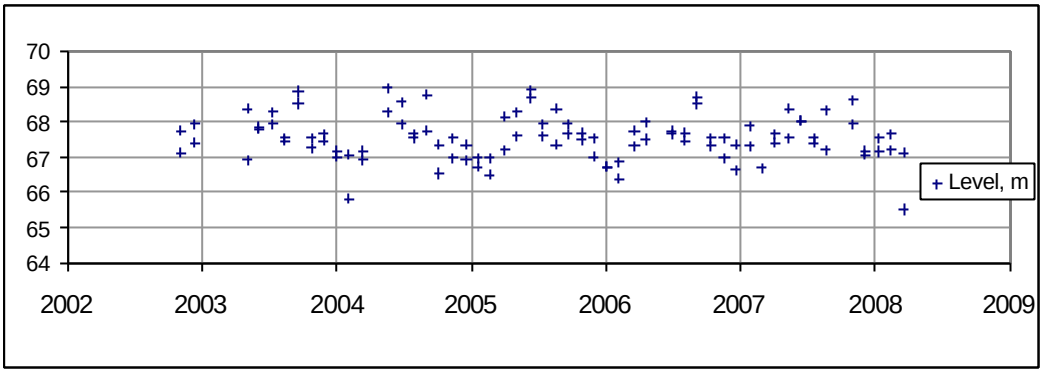

a)

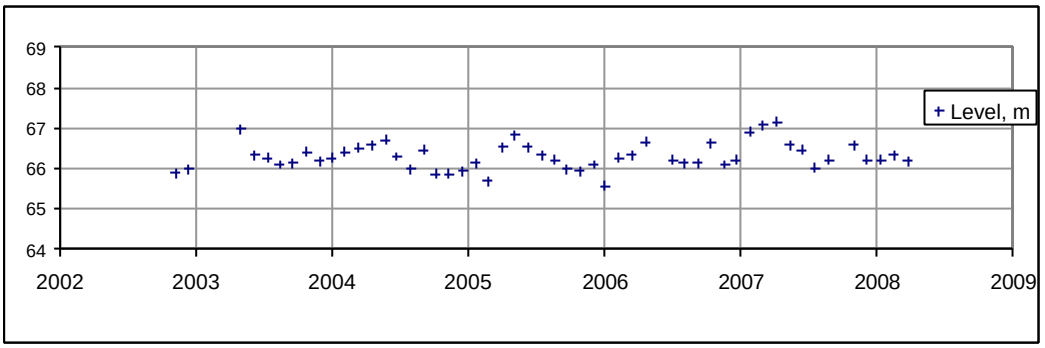

b)

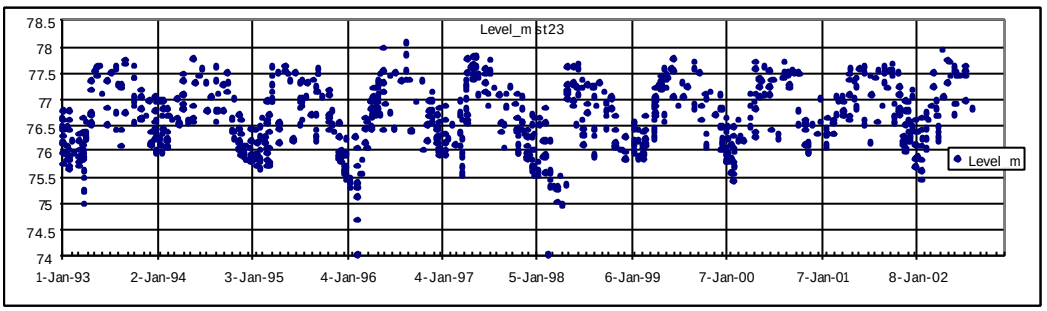

c)

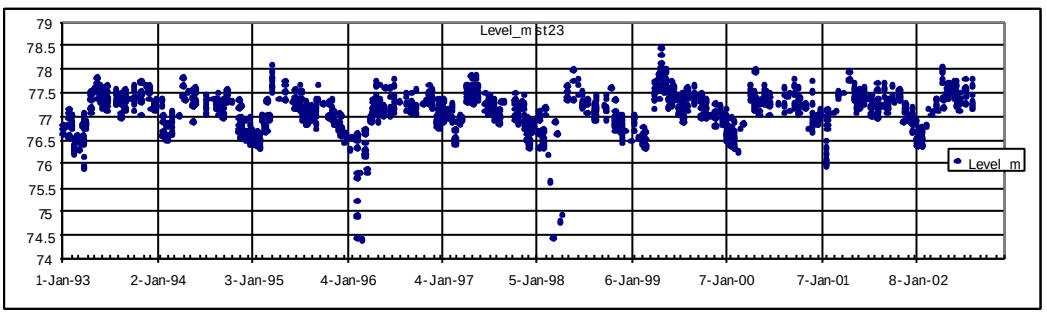

d)

Figure 8. Water level variability for Nadym swamps region: a - lake, b - drained lake (khasyrey) and Surgut swamp region: c - lake, d - flat bog.

4. Water level and river discharge of large Arctic rivers

4. Water level of large Arctic rivers

4.1. Ob' river (ENVISAT radar altimetry)

ENVISAT data (Ice2 retracker) have been used to identify 58 virtual stations (intersection of the satellite ground track and river channel) along the main channel of the Middle and Lower Ob' (Figure 9). Water level variability for each station is presented in the file "Ob river ENVISAT time series.xls" (directory /River Level/Ob/). The calculations are based on the processing of 18 Hz ENVISAT data using a fine geographical selection (using Landsat GeoCover imagery with 14.25 m spatial resolution). This dataset has been provided also as a contribution to the planned AltiKa radar altimetry mission (2011).

By averaging all values from 2002 to 2009 for each station, a spatial variability of maximal and minimal water level values, as well as amplitude has been calculated along the river (Figure 9, b). We observe a general decrease of both absolute values of water level (eroding effect of the river) and amplitude (widening of the river channel) toward the outlet. However variability along the river is also characterised by irregularities and spikes, that are related with several factors, such as river valley width, influence of confluents etc.

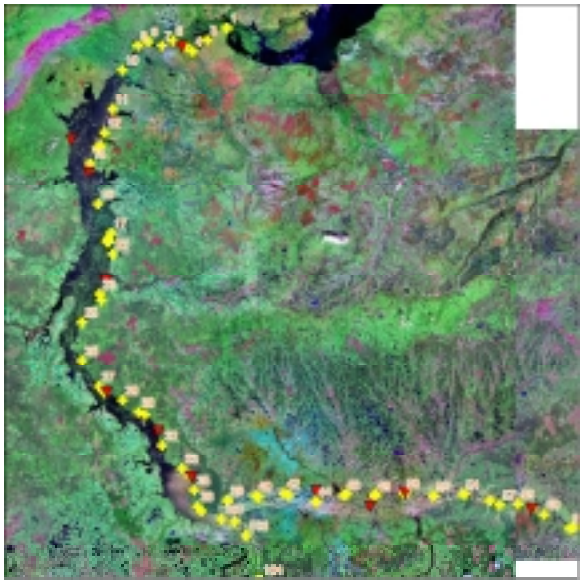

a)

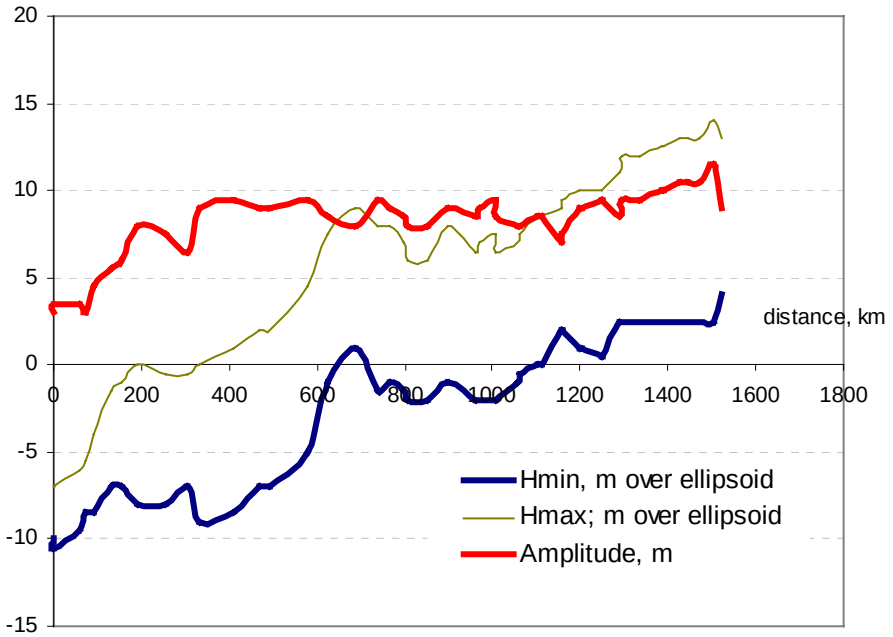

b)

Figure 9. Virtual stations over the Middle and Lower Ob' river (a) and water level variability (b) along the river (maximal and minimal values, as well as amplitude). Averaged data for 2002-2009. Distance is expressed in km starting from the northernmost virtual station.

4.2. Ob', Yenisey and Lena rivers (Hydroweb Vals processing)

Hydroweb database also provide water level variability for the three largest Eurasian arctic rivers: Ob' (27 virtual stations), Yenisey (33 stations) and Lena (21 stations) (Figure 10) using ENVISAT RA-2 radar altimeter. These data are presented as ASCII

files (one file per virtual station) in the directory /River Level/Hydroweb/River Name/ where "River Name" could be Ob, Yenisey or Lena.

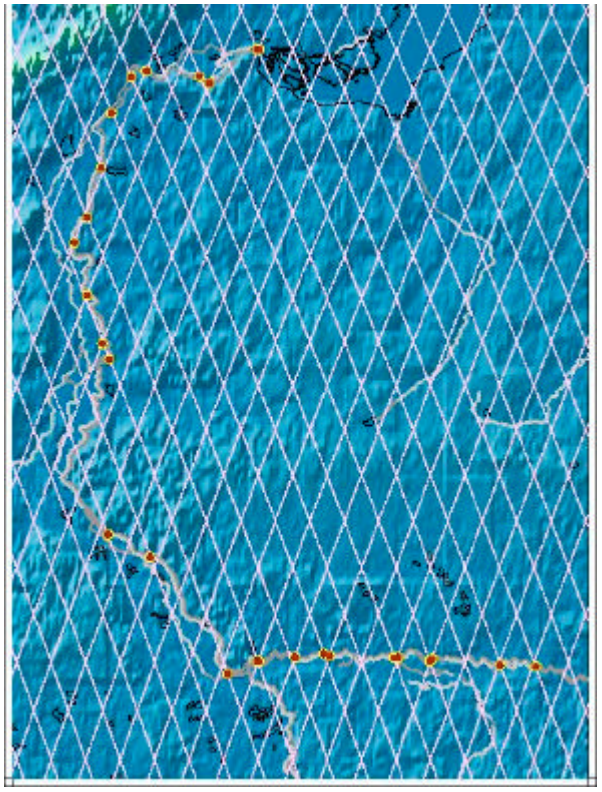
a)

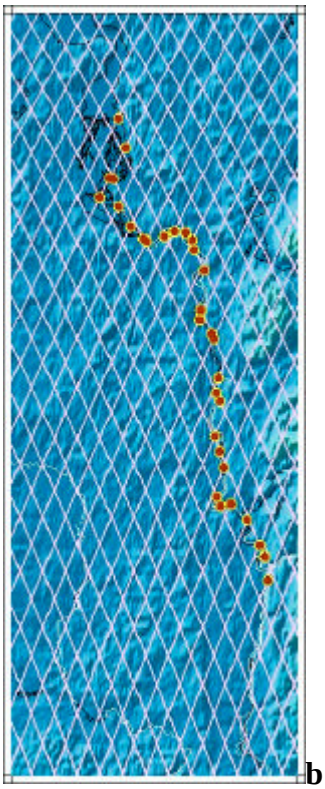
b)

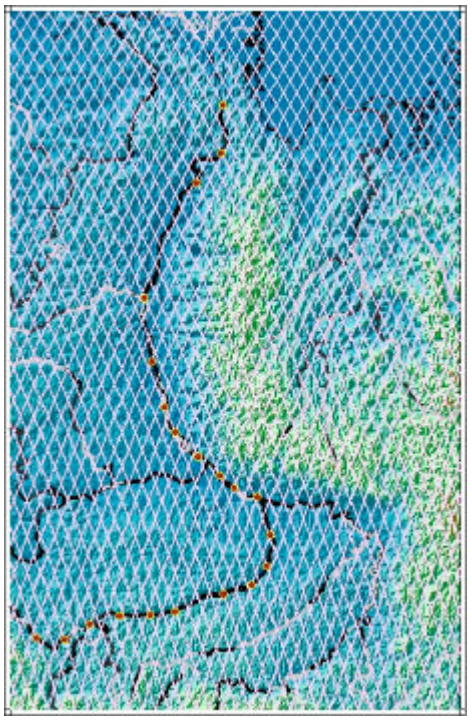
c)

Figure 10. Hydroweb virtual stations over the Ob' (a), Yenisey (b) and Lena (c).

4.3. Historical river level and discharge data (ArcticRIMS website)

ArctiRIMS web site (http://rims.unh.edu/index.shtml] provide information concerning daily and monthly values of river level and dicharge (Figure 11).

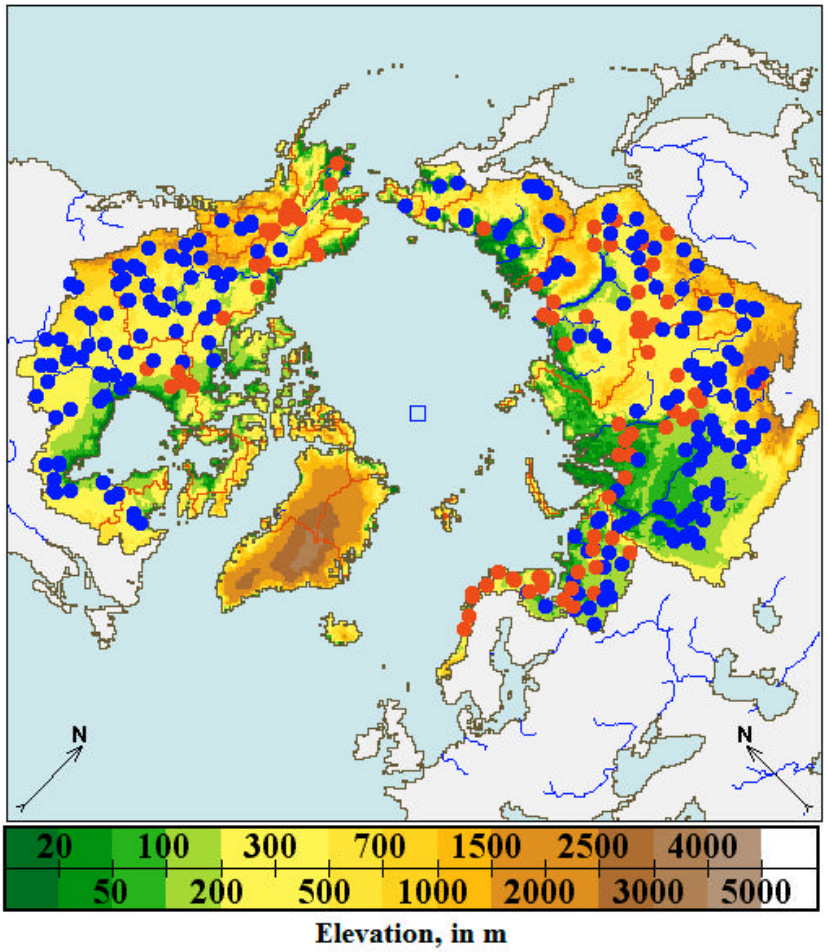

Figure 11. ArcticRIMS stations (red dots - operational, blue dots - re-analysis sites).

Most of the rivers flowing to the Arctic Ocean are presented there and users can download the data in ASCII format for each of the stations. The site also provide other relevant information such as watershed-based reanalysis data on temperature, precipitation etc.

Monthly data on river discharge (m3/s) and stage (water height, m) for the large Eurasian rivers and Yukon river are presented in the directory /ArcticRIMS/. Data for Canadian stations are not publicly available within ArcticRIMS (access is not granted to research, environment, and other public communities, and you need to contact Canadian agencies to get personal permission to access data).

Each river has its code (see table 2) and there could be several ASCII files for each river - archival discharge (pre-2000) - "AD", archival stage ("AS"), provisional (post 2000) discharge ("PS") and provisional stage ("PS"). File names are in the format YYYYYXX.dat, where YYYYY is the station code (variable length), and XX could be one of the four values (AD, AS, PD, PS).

Table 2. Rivers, observation station and station code

for which monthly data are presented.

River	Station	Code
Onega	Porog	70842
Severnaya Dvina	Ust' Pinega	70801
Pinega	Kulogory	70334
Mezen'	Malonisogorskoye	70884
Pechora	Ust'-Tsilim	70850
Ob'	Salekhard	11801
Nadym	Nadym	11805
Pur	Samburg	11807
Taz	Sidorovsk	11808
Yenisey	Igarka	9803
Anabar	Saskulakh	3801
Olenek	Suhana	3407
Lena	Kusur	3821
Yana	Yubileynaya	3861
Indigirka	Indigirskiy	3489
Kolyma	Kolymskoye	1802
Yukon	Pilot Station AK	15565447

4.4. Estimating river discharge from altimetric water level

River discharge can also be estimated by combining altimetric observations of water level and historical in situ data on river discharge. An example of such application for the is presented in Annex 2. One of the largest Eurasian rivers – the Ob' river – was chosen in order to estimate the accuracy of the T/P altimetric measurements of river level and discharge. Altimeter water levels have been retrieved during the various phases of the Ob' hydrological regime and relationships between satellite-derived water level and river discharge measurements at Salekhard gauging station near the Ob' estuary has been established. A simplified relation between the water level (H) and river discharge (Q) without the use of detailed in situ information on hydraulic and morphological particularities of the chosen river section is considered. This simplification is done in order to estimate the applicability of such an approach for conditions when such base information is not available. The calculated discharges are then compared with in situ measurements and an assessment of the accuracy of the altimeter discharge estimates is performed.

It has been found that altimetric river level data can successfully be used for hydrological studies of seasonally ice-covered Arctic rivers. The accuracy of the discharge estimation is good enough to estimate the daily discharges and the annual water flow with an average error of 8% and 1-3%, correspondingly. For the mean monthly discharges, the average errors increase up to 17%, mostly due to the scarcity of valid T/P observations during some periods and discharge overestimation during the water depletion period in August-October. The introduction of new retracking

algorithms for computing the river level will significantly increase the accuracy of the discharge estimates.

References

Aladin N, J-F Crétaux, I. S. Plotnikov, Kouraev A. V., A. O. Smurov, A. Cazenave, A. N. Egorov, F. Papa. "Modern hydro-biological state of the Small Aral Sea". Environmetrics, 2005, 16(4), pp 375-392

Birkett C. The contribution of TOPEX NASA radar altimeter to the global monitoring of large rivers and wetlands. Water Resources Research, 34, 1223-1239, 1998.

Birkett C. The contribution of TOPEX/POSEIDON to the global monitoring of climatically sensitive lakes, J. Geophys. Res., 100, 25179-25204, 1995.

Bjerklie D.M., Dingman S.L., Vorosmarty C.J., Bolster C.H., Congalton R.G. Evaluating the potential for measuring river discharge from space, Journal of Hydrology Volume 278, Issues 1-4 , 25 July 2003 , Pages 17-38.

Broecker, W. S., Thermohaline circulation, the Achilles Heel of our climate system: will man-made CO2 upset the current balance? Science 278, 1582 (1997).

Cazenave A., Bonnefond P., Dominh K., Shaeffer P. Caspian sea level from Topex-Poseidon altimetry: level now falling. Geophys. Res. Lett. 1999, 24, 881-884.

Crétaux J. F. and Birkett S., Surface waters from space: lakes. Geosciences Comptes Rendus, Académie des sciences, Thematic issue 'Observing the Earth from space', 2006, 1098-1112.

Crétaux, J-F, A.V. Kouraev, F. Papa, M.Bergé-Nguyen, A. Cazenave, N. Aladin, I.S. Plotnikov. "Water balance of the Big Aral Sea from satellite remote sensing and in situ observations". Journal of Great Lakes Research, 2005, 31(4), p. 520-534.

de Olivera Campos, Ilce, et al. Temporal variations of river basin water from TOPEX/Poseidon satellite altimetry. Application to the Amazon bason, Comptes Rendus de l'Académie des Sciences, Serie II, Sciences de la Terre et des planètes, 333, 1-11, 2001.

IPCC (Intergovernmental Panel on Climate Change), Climate Change 2001: The Scientific Basis. Contribution of Working Group to the Third Assessment Report of the PCC, J. T. Houghton et al., Eds. (Cambridge Univ. Press, Cambridge, 2001).

Kouraev A.V., Kostianoy A.G., Lebedev S.A. "Recent changes of sea level and ice cover in the Aral Sea derived from satellite data (1992-2006)". Journal of Marine Systems, 2008 doi:10.1016/j.jmarsys.2008.03.016 Available online 12 August 2008

Kouraev A.V., Zakharova E.A., Samain O., Mognard-Campbell N., Cazenave A. "Ob' river discharge from TOPEX/Poseidon satellite altimetry data", Remote Sensing of Environment, 93, 2004, pp. 238-245

Legrésy, B., & Rémy, F. (1997), Altimetric observations of surface characteris-tics of the Antarctic ice sheet. Journal of Glaciology, 43(144), pp. 265-275

Maheu C., Cazenave A.,. Mechoso C.R. Water Level Fluctuation in La Plata basin (South America) from TOPEX/Poseidon Satellite Altimetry. Geophysical Research Letter, 30, 3, 2003

Mercier F., Cazenave A., Maheu C. Interannual lake level fluctuations in Africa from Topex/Poseidon: connections with ocean-atmosphere interactions over the Indian ocean. Global and Planet. Change, 32, 141-163, 2002

Mercier, F. Altimétrie spatiale sur les eaux continentales: apport des missions TOPEX/POSEIDON et ERS-1&2 ? l'étude des lacs, mers intérieures et bassins fluviaux., PhD thesis, 2001, Université Paul Sabatier.

Papa F., C Prigent, F Durand, WB Rossow Wetland dynamics using a suite of satellite observations: A case study of application and evaluation for the Indian subcontinent. - Geophysical Research Letters, 2006

Peterson B.J., R. M. Holmes, J. W. Mc Clelland, C. J. Vo¨ro¨ smarty, R. B. Lammers, A. I. Shiklomanov, S. Rahmstorf. Increasing river discharge to the Arctic ocean, Science, 298, 21712173, 2002.

Ponchaut, F. and Cazenave, A. Continental lake level variations from TOPEX/POSEIDON (1993-1996). Earth and Planetary Sciences, 326, 13–20. 1998

Prigent C.,F. Papa,F. Aires,W. B. Rossow, and E. Matthews. Global inundation dynamics inferred from multiple satellite observations, 1993–2000. Journal of Geophysical research, VOL. 112, D12107, doi:10.1029/2006JD007847, 2007

Rahmstorf, S., 1995: Bifurcations of the Atlantic thermohaline circulation in response to changes in the hydrological cycle. Nature, 378, 145-149.

Shiklomanov, A.I., Lammers, R.B. and Vorosmarty C.J., Widespread decline in hydrological monitoring threatens Pan-Arctic research, EOS Trans.AGU, 83, 13-16, 2002.

Zakharova E.A., Kouraev A.V., Cazenave A, Seyler F. "Amazon river discharge estimated from Topex/Poseidon satellite water level measurements", Comptes Rendus - Geoscience, 2006, Vol 338, No 3, 188-196.

Annex 1. Influence of ice cover on altimetric water level measures

Kouraev A.V., Kostianoy A.G., Lebedev S.A. "Recent changes of sea level and ice cover in the Aral Sea derived from satellite data (1992-2006)". Journal of Marine Systems, 2008 doi:10.1016/j.jmarsys.2008.03.016 Available online 12 August 2008

Journal of Marine Systems 76 (2009) 272–286

Contents lists available at ScienceDirect

Journal of Marine Systems

journal homepage: www.elsevier.com/locate/jmarsys

Ice cover and sea level of the Aral Sea from satellite altimetry and radiometry (1992–2006)

Alexei V. Kouraev [a,b,*], Andrey G. Kostianoy [c], Sergey A. Lebedev [d,e]

[a] Université de Toulouse; UPS (OMP-PCA); LEGOS; 14 Av. Edouard Belin, F-31400 Toulouse, France
[b] State Oceanographic Institute, St. Petersburg Branch, Russia
[c] P.P. Shirshov Institute of Oceanology, Russian Academy of Sciences, Moscow, Russia
[d] Geophysical Center, Russian Academy of Sciences, Moscow, Russia
[e] State Oceanographic Institute, Moscow, Russia

ARTICLE INFO

Article history:
Received 5 February 2007
Received in revised form 10 February 2008
Accepted 12 March 2008
Available online 12 August 2008

Keywords:
Aral Sea
Sarykamysh Lake
Sea level
Ice cover
Satellite altimetry
Microwave radiometry

ABSTRACT

We discuss recent seasonal and interannual variations of ice cover and lake surface level in the Aral Sea from satellite data for 1992–2006. First, we provide an overview of the evolution of the Aral Sea's environmental conditions, hydrological and ice regime, existing observations and current state of the scientific research. Desiccation of the Aral Sea led to disappearance of the infrastructure in the coastal zone, including meteorological and sea level gauge stations. The current lack of reliable in-situ measurements and time series for sea level and ice cover parameters since mid-1980s can be partly overcome with radar altimeter and microwave satellite observations that provide reliable, frequent, regular and weather-independent data. In our study, we use radar altimeter data from TOPEX/Poseidon, Jason-1, ENVISAT and GFO satellites, as well as the Special Sensor Microwave/Imager (SSM/I) radiometer. An ice discrimination method, based on the synergy of active and passive data from the four altimetric missions and SSM/I, is proposed and applied to the entire satellite dataset to define the specific dates of ice events for 1992–2006. We then analyse the evolution of the sea level in the Large and Small Aral sea and Sarykamysh lake. For this purpose, we compare time series from several sources (Hydroweb, USDA Reservoir Database, Integrated Satellite Altimetry Data Base and others), perform an intercomparison of the available observations and discuss the reasons for potential differences. Using the data from the four altimetric retrackers for ENVISAT, we also estimate how the presence of ice could affect the altimeter range measures. We estimate the associated uncertainties and provide recommendations for adjusting sea level time series for altimeters where only ocean retracker (T/P, Jason-1, GFO) is present.

1. Introduction

Shallowing and degradation of certain freshwater and salt lakes and inland seas are major environmental problems at the beginning of the XXI century (Micklin, 1988; Létolle and Mainguet, 1993; Birkett, 1995; Micklin and Williams, 1996; Glantz, 1999; Mercier, 2001; Mercier and Cazenave, 2001; Mercier et al., 2002; Kostianoy and Wiseman, 2004; Kostianoy et al., 2004; Kostianoy, 2006). There are clear indications that the growth of human population and the increasing use and abuse of natural resources, combined with climate changes, exert a considerable stress on closed or semi-enclosed seas and lakes. In many regions of the world, marine and lacustrine aquatic systems are (or have been) subjects to severe or fatal alterations ranging from changes in regional hydrological regimes and/or modifications of the quantity or quality of water resources, deterioration of geochemical balances (increased salinity, oxygen depletion, etc.), mutations of the ecosystems (eutrophication, dramatic decrease in biological diversity, etc.) to geological disturbances and the socio-economic problems. Seas and lakes are endangered all over the world and some may be even regarded as already "dead".

* Corresponding author. Université de Toulouse; UPS (OMP-PCA); LEGOS; 14 Av. Edouard Belin, F-31400 Toulouse, France. Fax: +33 5 61 33 29 02.
E-mail address: kouraev@legos.cnes.fr (A.V. Kouraev).

0924-7963/$ – see front matter © 2008 Elsevier B.V. All rights reserved.
doi:10.1016/j.jmarsys.2008.03.016

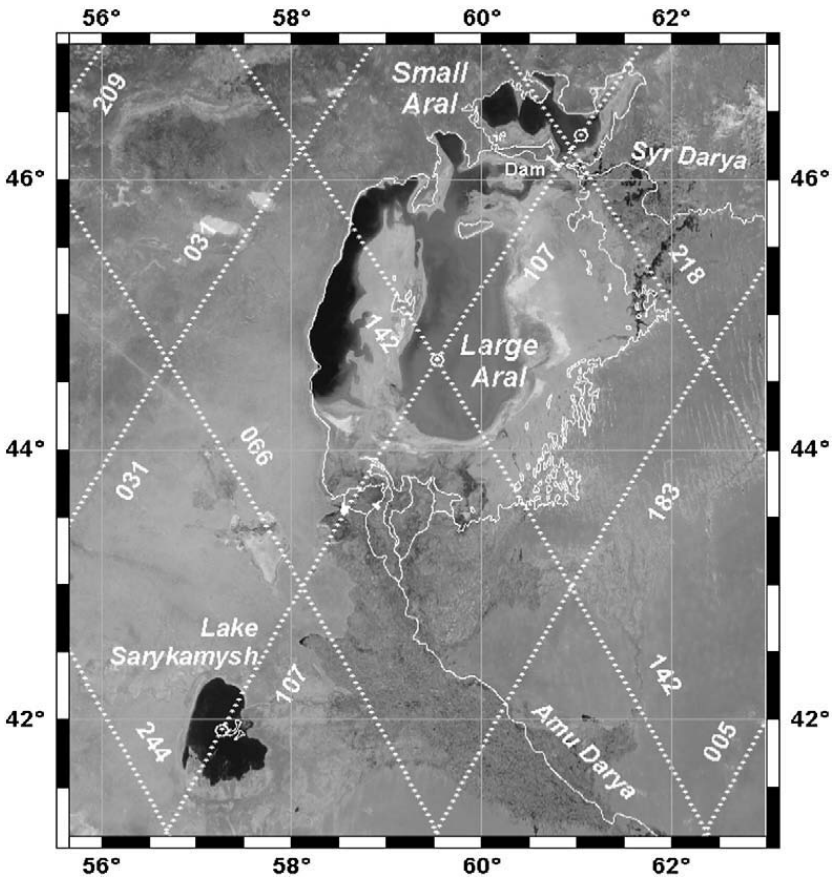

Fig. 1. The Aral Sea and Lake Sarykamysh in the MODIS image on 18 May 2002 (credit of Jacques Descloitres, MODIS Land Rapid Response Team, NASA/GSFC) with the T/P (since August 2002 replaced by Jason-1) ground tracks (dotted lines). Coastal line (solid white line) is shown for 1962 as well as Amudarya and Syrdarya Rivers. Circles show data points on the T/P tracks used for the analysis.

The most striking examples are the Lobnor Lake in China, which completely dried up by 1972, the Dead Sea, whose level has dropped by 14 m since 1977 and whose present salinity is about 340 g/l, the Aral Sea, whose level has dropped by about 23 m and whose salinity increased by a factor of 10 since 1960, and Lake Chad, which has shrunk to about one-twentieth of its size in 1963.

The Asia's closed and terminal lakes are located in arid or semi-arid regions and, therefore, are sensitive to changes in water balance. Thus, the lake levels and salinity react quickly on any regional climate change or anthropogenic pressure. Unsustainable irrigation in lake basins has already led to very serious environmental and social-economic problems. The lakes will be particularly vulnerable to any future reduction of

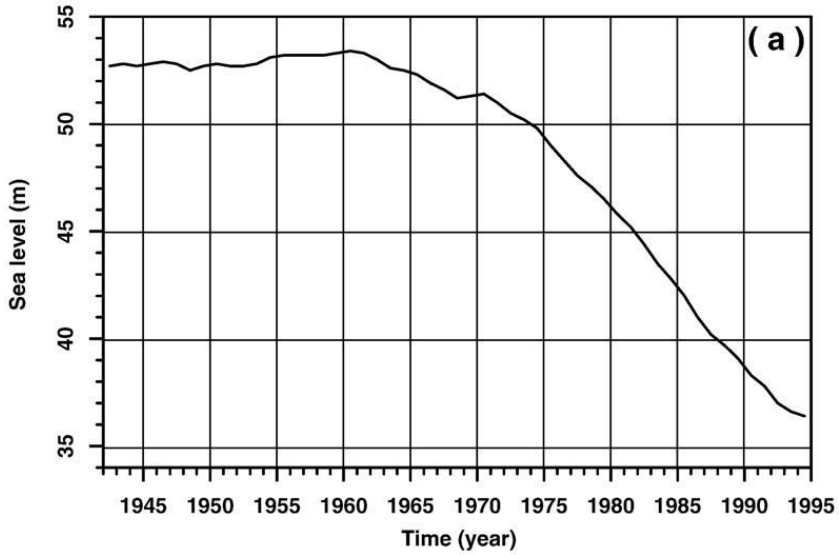

Fig. 2. Time variation of the Aral Sea level based on instrumental measurements for the period from 1943 to 1994 (Mikhailov et al., 2001).

precipitation over the catchment area or to temperature increase. We note that according to some global warming studies the future climate change in Central Asia is likely to be more abrupt than that in other regions.

The Aral Sea (Fig. 1) is one of the most striking examples of what unsustainable use of water can do to aquatic ecosystems (Micklin, 1988; Létolle and Mainguet, 1993; Glazovsky, 1995a,b; Micklin and Williams, 1996; Zonn and Glantz, 2008). Once the fourth largest inland water body with a surface area of over 66,000 km^2, a total volume of 1070 km^3 and a maximum depth of 69 m, in 1960. The Aral Sea had about the size of the Netherlands and Belgium taken together. Many fish species were living in the brackish water (mean salinity was about 10 g/kg), 12 of them were very important for fisheries (yearly catches of 44 000 tons on average). But over the past fifty years, the freshwater discharge into the Aral Sea from the Amudarya and Syrdarya rivers (formerly, over 50 km^3/yr) has been decreasing because of diversions for irrigation and ceased almost completely. As a result, the sea surface level (Fig. 2) has dropped by 23 m (in the Large Aral), the lake has shrunk by a factor of five from its original size and a factor of ten in its volume, the salinity exceeded 90 g/kg in the western Aral Sea (in 2006) and is even higher (130–150 g/kg) in the eastern part (Zavialov, 2005).

In 1989, the northernmost part and the main body of the lake separated, forming two individual lakes, known as the Small Aral Sea and the Large Aral Sea. At that moment, the lake level was about 39 m above the ocean level. Then, the AVHRR-NOAA satellite imagery allowed reconstructing the decrease of the Large Aral sea level: 1990 — 37.8–38.5 m, 1996 — 36 m, 1999 — 34 m. At the same time, the level of the Small Aral Sea oscillated between of 39 m and 42 m, due to construction and destruction of several dams between the two parts of the lake. The progressive changes of the Aral Sea shape are shown in Figs 1 and 4.

Today, the Aral Sea is divided in three almost separate parts (Figs. 1, 3 and 4). The Large Aral itself, due to the continuing sea level drop, presently consists of two distinct basins connected through a narrow and relatively shallow channel (Figs. 1, 3 and 4) since 1998 (Zavialov, 2005). The western basin is a trench with a steep bottom slope at the western side where the maximum depths still exceed 40 m, while the eastern basin is a relatively large but very shallow (less than 5 m deep) water body. The desiccation and salinization of the sea have led to desertification and degradation of the regional ecosystem, and had severe impact on the quality of life and health of the local population (Micklin, 1988; Létolle and Mainguet, 1993; Glazovsky, 1995a, b; Micklin and Williams, 1996; Glantz, 1999; Kostianoy and Wiseman, 2004; Mirabdullayev et al., 2004; Zavialov, 2005; Nezlin et al., 2005).

Lake Sarykamysh is a large drainage water body, located southwest of the Aral Sea (see Fig. 1). It was used as a discharge collector of salty irrigation water from the agricultural fields. In 1971, a unified lake has arisen as a result of joining of a group of ponds to form the Sarykamysh Lake. It has been long observed that on large temporal scales, the variability of Sarykamysh Lake volume was somewhat anti-correlated with that of the Aral Sea, because much of the water resources withdrawn from the Aral basin for irrigation are eventually drained into Sarykamysh. This is why the recent evolution of the Sarykamysh Lake is of interest in the general context of the Aral Sea crisis. Currently, the lake covers an area exceeding 3000 km^2 and its maximum depth is about 45 m. The salinity of the lake waters has been continuously increasing: from 3–4 g/l in the early 1960s to 12–13 g/l in 1987 (Glazovsky, 1995b). Direct water level measurements by level gauges for this lake are lacking to the present time.

The Aral Sea is located on the far southern boundary of the sea ice cover development in the Northern Hemisphere, but every winter it is covered by ice for several month (Fig. 3). Due to this marginal location, data on ice variability in the lake may serve as a proxy of the regional and even large-scale climate change. Ice processes in the Aral Sea have a significant temporal and spatial variability, influenced by severity of winters, meteorological conditions, wind fields, as well as by sea morphology and steadily increasing salinity. So far, most

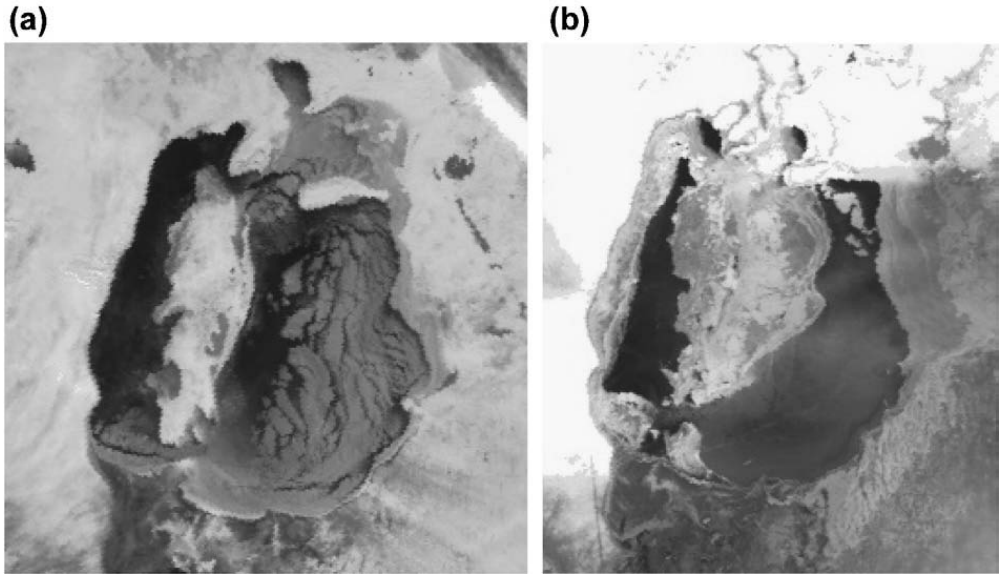

Fig. 3. The Aral Sea ice conditions derived from NOAA visible imagery: (a) appearance of ice on 14 December 1995, (b) disappearance of ice in the southern part of the Large Aral Sea on 5 March 1989 (credit of D. Soloviev, Marine Hydrophysical Institute, Sevastopol, Ukraine).

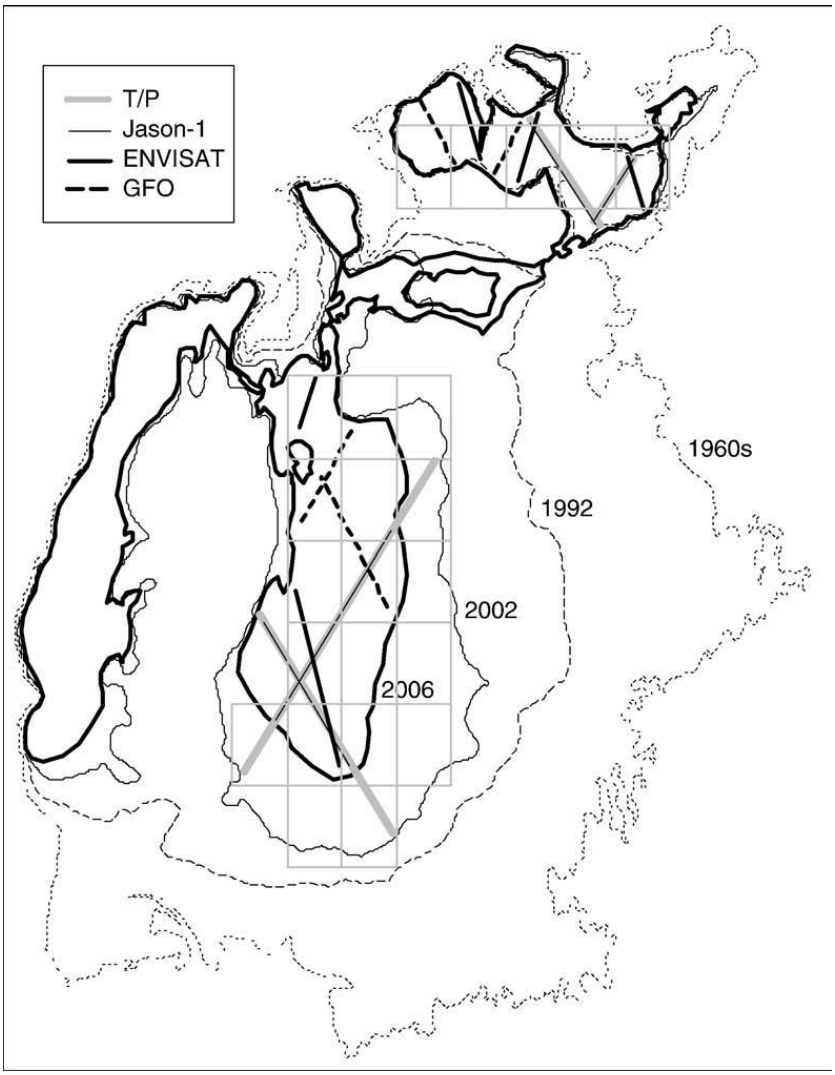

Fig. 4. Position of the coastline of the Aral Sea in 1960, 1992, 2002 and 2006, and selected altimetric satellite ground tracks and EASE-grid pixels of SSM/I observations (grey rectangles).

of the publications on historical variability of ice conditions of the Aral Sea were in Russian (see Kosarev, 1975; Bortnik and Chistyayeva, 1990 for a detailed overview) and thus remain inaccessible for many western readers (Nihoul et al., 2002). A brief overview of historical ice conditions of the Aral Sea in English can be found in (Kouraev et al., 2004a, Kostianoy and Kosarev, 2005).

Sea level, ice conditions, and other meteorological and oceanographic parameters in the Aral Sea were under regular control at up to a dozen coastal meteostations (Bortnik and Chistyayeva, 1990). Regular ice observations in the Aral Sea at coastal stations begun in 1941 and those by means of aerial surveys started in 1950. They were done on a regular basis and, up to 1985, a total of 241 aerial surveys were carried out (Bortnik and Chistyayeva, 1990). Since the late 1970s, the frequency and amount of aerial surveys in the Aral Sea sharply decreased, due to financial problems as well as to general degradation of the sea related with rapid sea level fall. Since mid-1980s, the observations became less regular and, in many instances, the obtained results still reside in local archives unavailable for public. Moreover, the Aral Sea in its present limits is physically difficult to access for oceanographic and meteorological measurements.

However, the current lack of time series for sea level and ice cover parameters may be largely compensated for by satellite observations. Numerous studies have been using satellite imagery to estimate the evolution of the Aral Sea shoreline, and then deduce variability of the lake level. Direct satellite measurements of the lake level are possible from radar altimetry, which provide reliable, regular and weather-independent data. Several satellite altimetry missions have been launched since the early 1990s, namely, ERS-1 (1991–1996), TOPEX/Poseidon (P/T) (since 1992), ERS-2 (since 1995), Geosat Follow-On (GFO, since 2000), Jason-1 (since 2001) and ENVISAT (since 2002). Although the primary mission of satellite altimetry was the study of water level of the open ocean, this technique has been successfully applied to monitor water level of inland seas and lakes (Crétaux and Birkett, 2006). Application of satellite altimetry for monitoring of the Aral Sea level has been used in several research papers that are discussed below.

Peneva et al. (2004) have used T/P data for 1993–2001 to analyse the level and volume changes in the Large Aral Sea, estimate the influence of ground water inflow on water budget, and assess salt balance of the sea. Stanev et al. (2004) have used the same dataset to monitor the level in both Large

and Small Aral seas. Aladin et al. (2005) have used T/P and Jason-1 data for 1992–2003 to monitor variations in the level and volume of the Small Aral sea and estimate influence of various components on the water budget. Detailed assessment of the influence of the dam in the Berg strait on the sea level and evolution of the biological communities were also made by these authors. Crétaux et al. (2005) used T/P and Jason-1 data for 1992–2004 to estimate the lake level and volume changes of the Large Aral Sea and introduce variations of the lake volume as the new constraint for the water budget. They also discuss changes in the aquatic fauna and its possible evolution under continuing desiccation of the Large Aral Sea. Water level variability in the Lake Sarykamysh has been presented by (Mercier, 2001) and (Mercier and Cazenave, 2001).

Recent evolution of the Aral sea ice cover using satellite altimetry and radiometry was investigated by (Kouraev et al., 2003, 2004a,b). A methodology for discriminating the ice and open water using simultaneous active (radar) and passive (radiometer) from T/P was proposed, validated and applied for the Caspian and Aral seas. Detailed assessment of how different footprints of T/P sensors, and radiometric properties of water, ice and snow influence the proposed ice/water discrimination method is given in (Kouraev et al., 2004b). In (Kouraev et al., 2003), data from the two T/P tracks over the Large Aral Sea for 1992–2002 was used to estimate a) dates of the ice formation and break-up, b) ice duration and c) percentage of ice presence in the altimetric data. In (Kouraev et al., 2004a,b), the T/P data were complemented by the SSM/I observations with a dedicated ice/water discrimination approach. Using the satellite datasets for Large Aral, two separate time series of the ice formation and break-up and ice duration have been obtained. Ice presence has also been calculated as the percentage of ice in the altimetric data (same as in Kouraev et al., 2004b) and also as the total and maximal numbers of ice pixels for various sub-regions of the Large Aral Sea.

In this article, to provide a more comprehensive study of the ice cover, we a) complement the T/P observations by Jason-1, GFO and ENVISAT data, and b) use an improved ice discrimination approach combining all altimetric and SSM/I data (Kouraev et al., 2007a) and thus provide better spatial and temporal resolution. Using this approach, we derive new improved time series of ice events (ice formation, break-up and duration) for the longest possible period (1991–2006) for both Large and Small Aral Sea. We analyse the differences in ice events between the two basins and discuss possible reasons.

For the water level of large water bodies, currently there exist several sources of altimetric series that are publicly available online (Hydroweb, USDA Reservoirs database, Lakes and Rivers database). Basing on the same initial altimetric data, each group of researchers uses different methods to estimate the resulting water level for the given period (see Section 2.1 for more details). In this article, we complement the time series from these databases by yet another source of the altimetric data, i.e., the observations from the Integrated Satellite Altimetry Data Base (ISADB) developed in the Geophysical Center of the Russian Academy of Sciences (Medvedev et al., 1997). We perform an intercomparison of the observations and discuss the reasons for potential differences, taking the Large and Small Aral Seas, and Sarykamysh lake, as instructive examples. Using the data from the four altimetric retrackers for ENVISAT, we also estimate how the presence of ice could affects the sea level estimates for altimeters with the only ocean retracker (T/P, Jason-1, GFO).

2. Ice cover

2.1. Data

2.1.1. Satellite altimetry data

We used data from several radar altimetry missions (Fig. 5). The earliest data are available from the TOPEX/Poseidon (T/P) satellite, operated since 1992 and followed by Jason-1, orbiting on the same ground track since February 2002. We complement the T/P and Jason-1 data by observations from recent radar altimeters onboard Geosat Follow-On (GFO, in operation since January 2000) and ENVISAT (in operation since November 2002) satellites.

All of the four altimeters have two main nadir-looking instruments – a radar altimeter and a passive microwave radiometer – that provide simultaneous active and passive microwave observations from the same platform. The repeat period is 10 days for T/P and Jason-1, 17 days for GFO and 35 days for ENVISAT. The altimetry data were obtained from the Centre for Topographic studies of the Oceans and Hydrosphere (CTOH) at the LEGOS Laboratory.

2.1.2. Passive microwave data

The passive microwave data from SSM/I (Special Sensor Microwave/Imager) onboard the DMSP (Defence Meteorological Satellite Program) series are available since 1987. The National Snow and Ice Data Center (NSIDC) provided the SSM/I data mapped onto an Equal-Area Scalable Earth Grid (EASE-Grid) projection with 625 km^2 spatial resolution (Armstrong et al., 2003). The initial data were averaged to obtain pentad (5-day) mean values to provide continuous spatial coverage. We used the SSM/I data starting from the beginning of the T/P mission in 1992.

2.1.3. Geographical selection

We performed a geographical selection of the data in order to minimise the potential contamination of the altimetric and SSM/I signal by land reflections. For the Aral Sea which experiences large changes in the position of the coastline, we used several masks to exclude the altimetry data that are 1 km or closer to the coast. In order to account for the lowest possible sea level, for T/P we selected data using the coastline position of 2002, i.e., the time when T/P has been put to a new orbit (Fig. 4), and for Jason-1, GFO and ENVISAT we used the coastline position obtained from a Landsat image taken on 26 October 2006. For the SSM/I data, we used the EASE-grid pixels if less than 30% of the pixel covers coastal regions or islands. In order to increase data availability, for Small Aral we kept some pixels that do not satisfy this condition, but used them with extreme caution. The data provide information for two regions: Small Aral and the eastern part of Large Aral. For the western part of the Large Aral, there were not enough data to obtain reliable estimates of the surface type.

2.2. Ice discrimination approach

In order to discriminate ice from open water, we used an algorithm developed for simultaneous active and passive

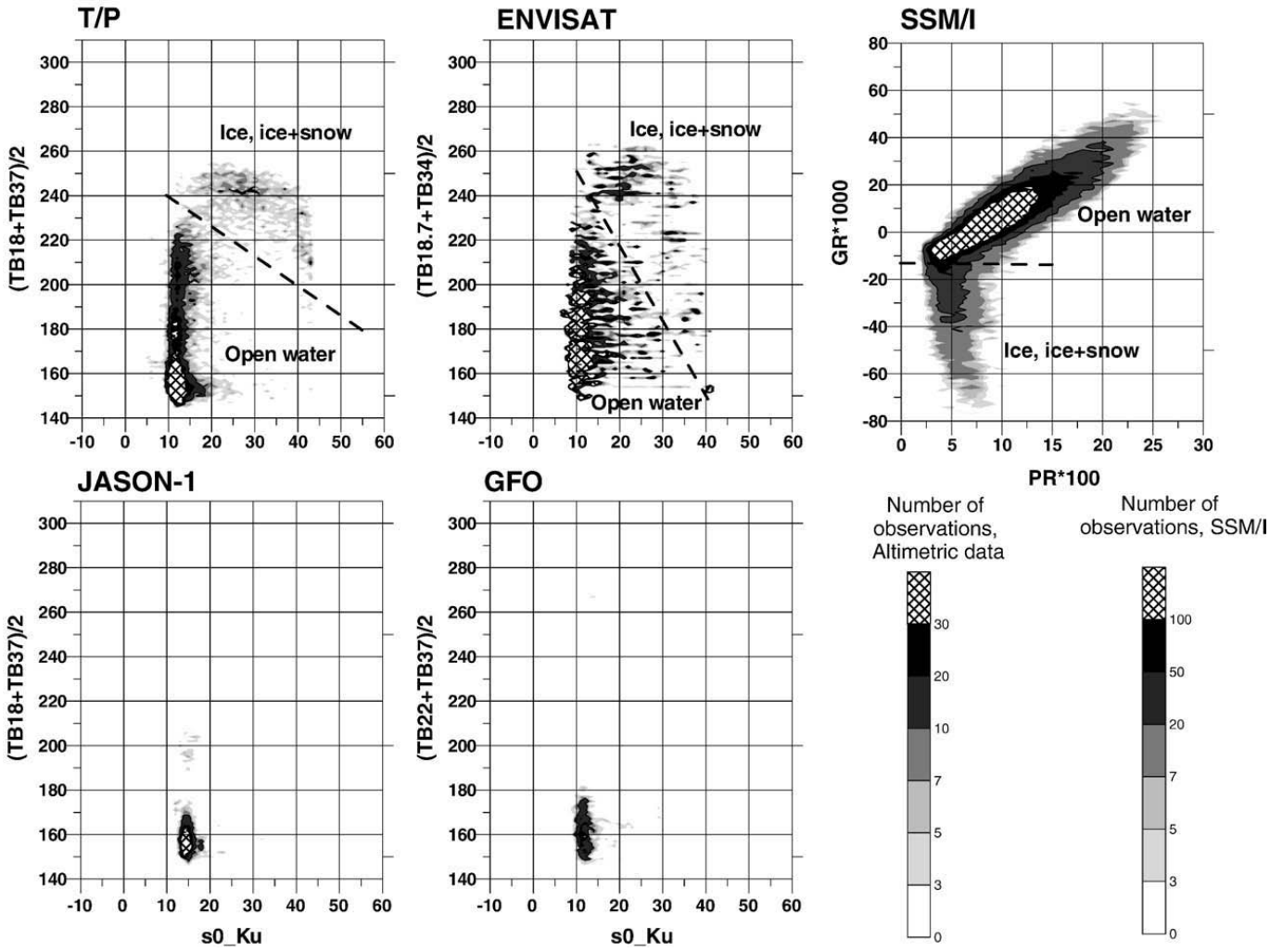

Fig. 5. Two-dimensional histograms (number of cases) of altimetric and SSM/I observations for Aral Sea for 1992–2006. For altimetric data the axes show the radar backscatter coefficient in Ku band (13.6 GHz) versus the average value of radiometer brightness temperature at two frequencies (depending on satellite). For SSM/I distribution is given in the polarisation (PR) and spectral (GR) gradient ratios space. Two main clusters (open water and ice/ice+snow) are shown, as well as the limits to separate open water and ice used in this study (dashed lines).

microwave data from T/P altimetric data and passive microwave data from SMM/I and applied for the Caspian and Aral seas (Kouraev et al., 2003, 2004a,b) as well as for the Lake Baikal (Kouraev et al., 2007a,b). For the Aral Sea, this method so far has been used only for the T/P data and for SSM/I data separately. In this work, we apply it to a wide range of the existing satellite radar altimetry missions, i.e., T/P, Jason-1, ENVISAT and GFO, and use a new approach using a series of consecutive maps for data analysis (Kouraev et al., 2007a).

2.2.1. Simultaneous active and passive microwave data from satellite altimetry

The ice discrimination method described in detail by (Kouraev et al., 2003, 2004b, 2007a) is based on the spatial-temporal evolution of the two parameters. The first parameter is the backscatter coefficient at Ku band (13.6 GHz), and the second parameter is the average value of the brightness temperature values at two frequencies, measured in °K, which we call "TB2". Open water has a low backscatter coefficient and low brightness temperature values, while ice cover is characterised by a high backscatter coefficient and elevated brightness temperatures. Using a set of threshold values for the backscatter and TB2, we can distinguish between open water and ice with a high degree of reliability, compared with using either parameter alone.

For T/P, Jason-1, and GFO, the backscatter and brightness temperatures values are provided for every 1 Hz data, thus giving an along-track ground resolution of about 6 km. For ENVISAT we use 18 Hz backscatter values from the Ice2 retracker (450 m resolution along the ground track). Observations from T/P and ENVISAT reveal two distinctive clusters (Fig. 5), representing open water and ice, what is typical for many seasonally ice-covered seas and lakes, such as the Caspian and Aral seas (Kouraev et al., 2003, 2004a,b), the Lake Baikal (Kouraev et al., 2007a) and others. The fact that for ENVISAT we have the backscatter value for every 18 Hz data and brightness temperature only for every 1 Hz data results in some stripes on the diagram. For Jason-1 and GFO data with high backscatter and TB2, the values are filtered out by the distributing agencies in the initial Geophysical Data Records (GDRs), which reduces its temporal resolution for estimating the timing of ice formation and break-up. In this study, we used Jason-1 and GFO data to reliably detect the open water.

2.2.2. Passive microwave data from SSM/I

Passive microwave data have been widely used to estimate both ice concentration and type for the Arctic and Antarctic sea ice (Ulaby et al., 1986; Steffen et al., 1992). The most commonly used algorithms for estimating the ice cover concentration from the passive microwave data are the NASA Team and Bootstrap algorithms (Swift and Cavalieri, 1985; Comiso, 1986; Steffen et al., 1992). These algorithms use various combinations of brightness temperature (TB) data from the 19.35 and 37.0 GHz horizontally (*H*) and vertically (*V*) polarised channels, such as the NASA Team algorithm where the polarisation (PR) and spectral gradient (GR) ratios are used.

Ice discrimination using passive microwave techniques requires a good knowledge of the radiometric properties of the ice for each specific natural object. For the present day Aral Sea, such data is absent. Moreover, while for the altimetry data open water and ice form two well defined and easily separated clusters, for SSM/I it is sometimes difficult to distinguish between the ice and water (see Fig. 5). Currently we apply a fixed GR ratio in order to distinguish between the ice and open water.

2.3. The recent Aral sea ice variability

The two types of observations have specific advantages, i.e., wide spatial coverage and good temporal resolution for the SSM/I and high radiometric sensitivity and along-track spatial resolution for the altimetry. The whole altimetric and SSM/I dataset has been processed using the ice discrimination methodology described by (Kouraev et al., 2007a). This methodology uses sets of threshold values to classify satellite data on the ice/water classification map for each pentad. We then analyse sequences of classification maps for each pentad to define the dates corresponding to the various ice cover events.

Compared to previous results (Kouraev et al., 2003, 2004a,b), this time we use a much larger dataset (including data from Jason-1, GFO and ENVISAT) for more extended period of time (1991–2006). Using the new ice discrimination methodology with better spatial and temporal resolution, we provide uniform time series based on the observations from several satellites instead of satellite-specific time series, for both Large and Small Aral Seas.

Using the methodology described above, we have defined dates of the ice formation (appearance of the first ice) and ice break-up (full open water observed) for the Large and Small Aral Seas for 1991–2006, except the winter 2003/2004 when, due to poor altimetric data coverage and availability, it was difficult to reliably define these dates for the Large Aral Sea. The variability of ice formation dates (Fig. 6a) is similar for both the Large and Small Aral Seas. On average, ice starts to

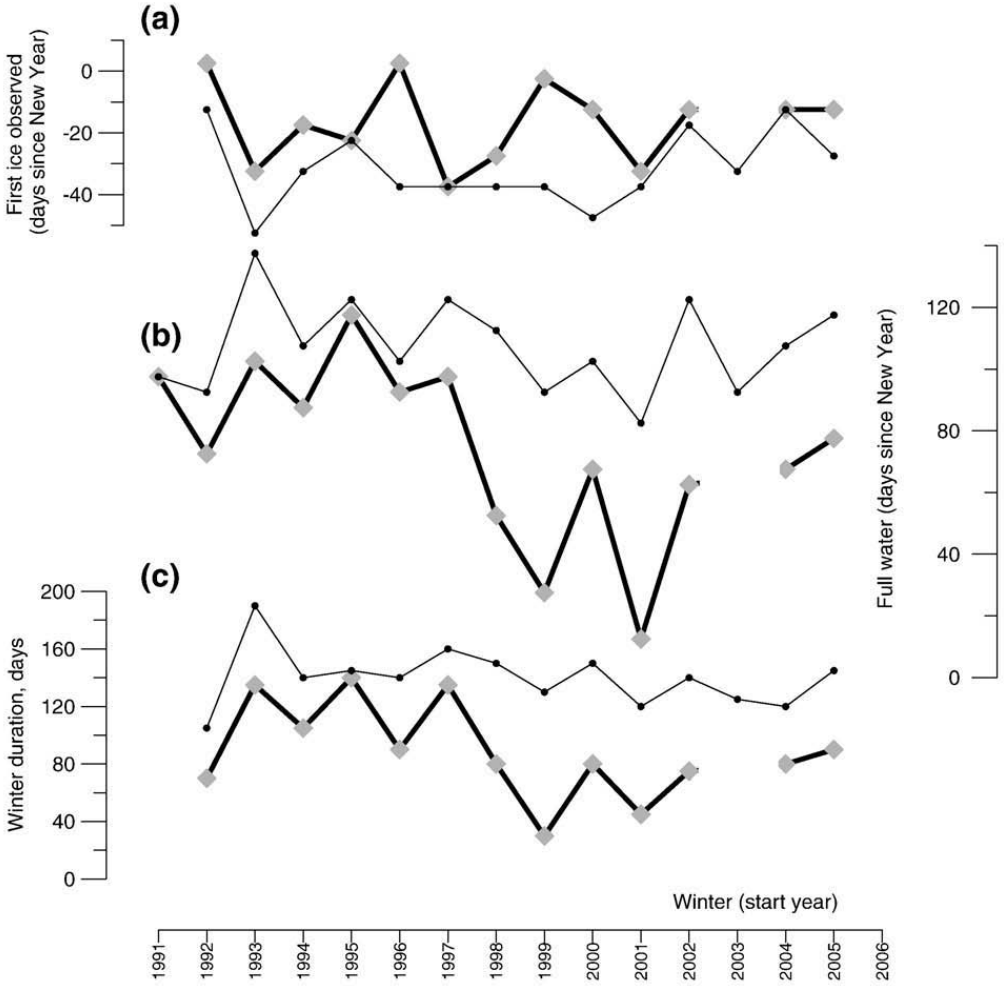

Fig. 6. Interannual variablity of ice event dates: (a) ice formation (first ice observed), (b) ice break-up (full open water), and (c) winter duration (difference between the two dates). Thick line — the Large Aral, thin line — the Small Aral. These data are also available online at the Hydroweb website.

form first in the Small Aral Sea and then it appears in the Large Aral Sea some 15 days later. For the ice break-up (Fig. 6b) the sequence of mild and severe winters is well seen both for the Large and the Small Aral Seas. However, the difference between the ice break-up dates for the two water bodies shows significant changes: for 1992–1997, the mean difference was 18 days, but since 1998 this value increased and the mean difference more than doubled to 50 days, with maximal value of 70 days. This rapid change is also evident in the "winter duration" (i.e., ice cover duration) time series (Fig. 6c). For the Small Aral Sea, the winter duration is stable around 140 days, while for the Large Aral Sea, this value decreased from 112 days in 1992–1997 to 69 days for 1998–2006.

Such a rapid shortening of the winter ice cover could be attributed to several factors. The variability of sea level results in changes of surface and volume, and thus of heat storage capacity. While for the Small Aral Sea the sea level has been stabilised, for the Large Aral Sea level decrease is continuing (Aladin et al., 2005; Crétaux et al., 2005; Zavialov, 2005). Using the dedicated Digital Bathimetry Model (DBM) of the Aral Sea (Crétaux et al., 2005) and altimetric series of the sea level we have estimated changes in the mean depth (defined as ratio of sea volume to sea surface) for the Eastern part of the Large Aral Sea and for the Small Aral Sea. While for 1992–2006 for the Small Aral this value was relatively constant — between 7.1 and 8 m, for the eastern Large Aral Sea mean depth has decreased almost three times: from 5.1 to 1.9 m. Another issue is the continuing increase of salinity of the Large Aral Sea. Before the separation of the Small and Large Aral Seas in 1989 the salinity was 28–30 ppt. Salinity measurements in the Large Aral Sea are sparse and not well assessed, but it is known that salinity in the Large Aral Sea has reached in 2002 more than 80 g/l (Zavialov et al., 2003a,b) in the western part and around 100–120 g/l in the eastern part in 2001 (Mirabdullayev et al., 2004). This change in salinity resulted in the decrease of the freezing temperature down to about −5 °C (Zavialov, 2005), but also in the lowering of temperature of maximal density, which, according to some data, even at 40–50 g/l becomes less than the freezing temperature (Ginzburg et al., 2003). Thus, during the autumnal cooling the sea is strongly stratified and cold surface layer does not sink downward. This might explain the fact that we do not observe significant difference in the timing of ice formation between the Small and Large Aral Sea. On the other hand, high salinity of the Large Aral lead to the development of thinner ice cover, and in spring this ice is more easily melted, what is proven by much earlier ice break-up in the Large Aral Sea comparing to the Small Aral Sea. An interpretation of the obtained series of ice conditions in the context of changes of both natural conditions and air temperature remains for the future.

3. The Aral Sea and lake Sarykamysh level variability

3.1. Altimetric time series used

The methodology of analysis of the water level variations based on the satellite altimetry data is considered in numerous publications (e.g., Morris and Gill, 1994a,b; Birkett, 1995, 1998; Larnicol et al., 1995; Cazenave et al., 1997; Mercier, 2001; Lebedev and Kostianoy, 2005). For the Large and Small Aral Seas and for Sarykamysh 3ake, currently, there exist several sources of altimetric series that are publicly available online (Hydroweb, USDA Reservoirs database, Lakes and Rivers database). We complement these existing time series by another source of altimetric data (ISADB), not available online. Departing from the initial altimetric data, different groups of researchers use specific methods to estimate the resulting sea level for the given period, and for this reason, we perform an intercomparison of the available observations on the example of Large and Small Aral Sea, and Sarykamysh Lake, and discuss the potential reasons for differences.

3.1.1. Hydroweb (Hydroweb web site, 2007)

This altimetric water level data base at LEGOS (Laboratory of Space Geophysics and Oceanography), Toulouse, France, contains time series encompassing water levels of large rivers, lakes and wetlands around the world. These time series are mainly based on the altimetry data from T/P for rivers, but ERS-1 and ERS-2, Envisat, Jason-1 and GFO data are also used for lakes. At present, water level time series for about 100 lakes and 250 sites (called virtual stations) on large rivers are available. The altimeter range measurements used for lakes consist of 1 Hz data. For large water bodies, the satellite data should be averaged over long distances and it is necessary to correct for the slope of the geoid (or, equivalently, the mean lake level). Because the reference geoid provided with the altimetry measurements (e.g., EGM96 for T/P data) may not be accurate enough, a mean lake level is computed, averaging the altimetry measurements themselves over time. The water levels are further referred to this 'mean lake level'. For the Large and Small Aral seas, the mean level is provided on the base of T/P, Jason-1, GFO and ENVISAT observations, and that for the Sarykamysh lake is derived from T/P, GFO and ENVISAT [J.-F. Crétaux, pers. comm.]. Each satellite data set is processed independently and potential radar instrument biases between different satellites are removed using the T/P data as a reference. Then the lake levels from the different satellites are merged on a monthly basis.

3.1.2. USDA reservoir database (USDA Reservoir database web site, 2007)

The U.S. Department of Agriculture's Foreign Agricultural Service (USDA-FAS), in co-operation with the National Aeronautics and Space Administration, and the University of Maryland, are monitoring lake and reservoir height variations for about 100 lakes worldwide using T/P and near-real time Jason-1 data. For the Aral Sea, the height variations are computed with respect to a 10-year mean level derived from T/P altimeter observations and are provided with 10 days resolution without median filtering.

3.1.3. ESA River and Lake (ESA River and Lake web site, 2007)

Since 2005, a new pilot system was launched at the European Space Agency (ESA) in ESRIN with the aim of deriving river and lake heights over Africa in near real-time using the ENVISAT data. Historical time series for 1995–2003 have also been generated over the African rivers and lakes using the ERS-2 data. This next release of this system should incorporate targets over the South and Latin America. Currently, there are several short time series (2006–2007) of the water level for various targets in the Aral Sea region

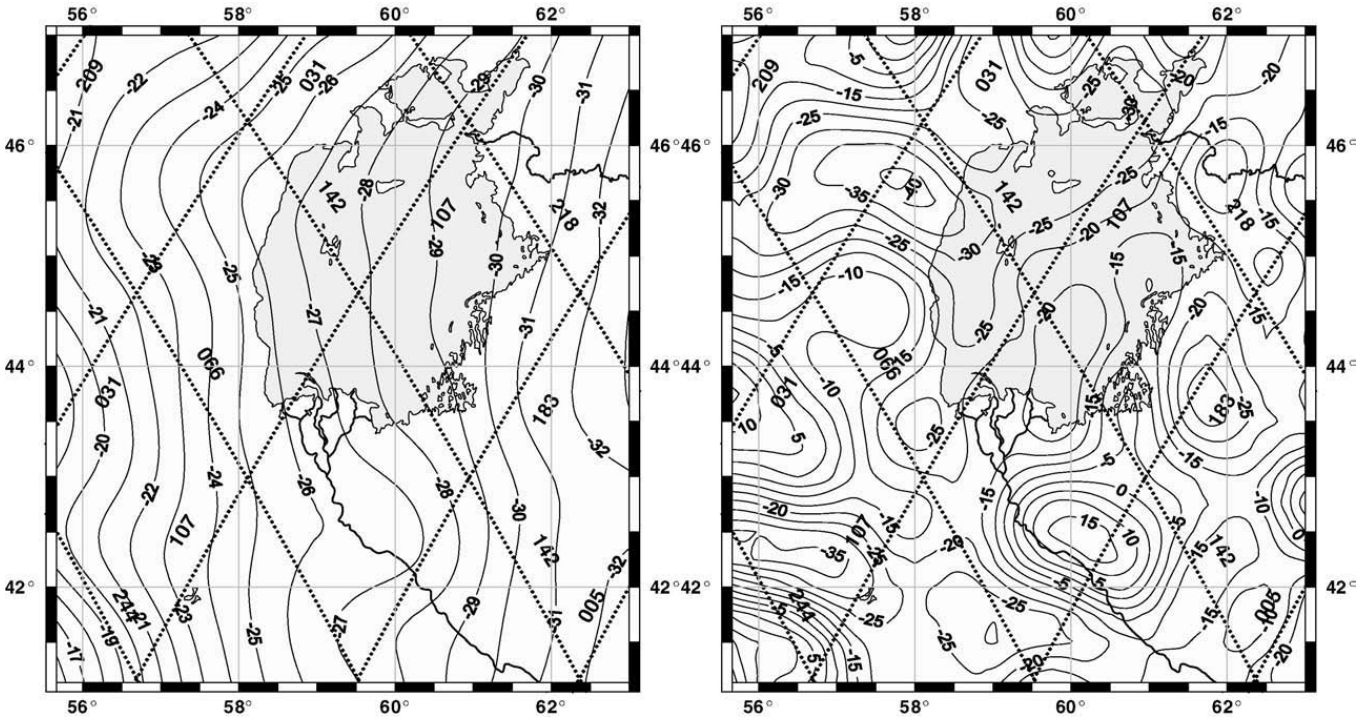

Fig. 7. Geoid height (left panel) and gravity anomalies (right panel) from the EGM96 model with decomposition on spherical harmonics 360°.

from ENVISAT data (accessible in the near real-time mode). However, for the Large Aral Sea, only 1 out of 12 available targets was actually over the sea, while the others are over the newly dry bottom (7 points), or located too close to the coast (4 points) to be reliable. The only point over the sea is in the Large Aral Sea and its short time series (3 cycles) show an increase of about 80 cm, while Hydroweb and USDA RDB both show a decrease of 20–40 cm for the same period. For the Small Aral Sea, 1 out of 4 available points is on land, and 3 others with time series of 4 to 6 cycles are noisy and not consistent with each other. For Sarykamysh there are 3 targets showing reasonable variability and trends comparable with those of Hydroweb, but the length of the series is too short (4 cycles). Due to all this, the data from the ESA River and Lake base are not used in this study.

3.1.4. Integrated Satellite Altimetry Data Base (ISADB)

This database has been developed at the Geophysical Center of the Russian Academy of Sciences (Medvedev et al., 1997). The satellite altimetry data of T/P and Jason-1 from the NASA Goddard Space Flight Center (GSFC) Ocean Altimeter Pathfinder Project (Koblinsky et al., 1999) were used. In addition, the T/P merged geophysical data records (MGDR) and Jason-1 interim geophysical data record (IGDR) and geophysical data records (GDR) were obtained from the NASA Physical Oceanography Distributed Active Archive Center

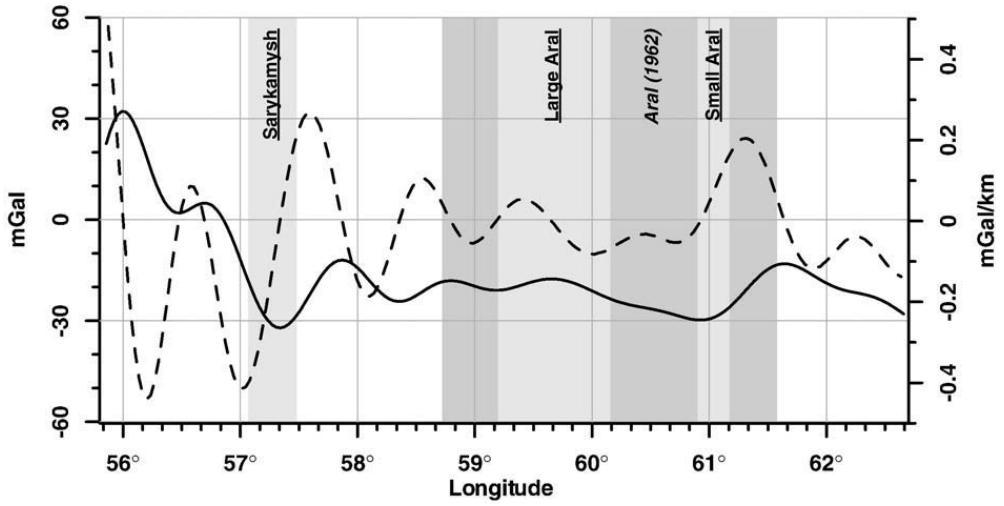

Fig. 8. Gravity anomaly (solid line) and its gradient (dashed line) along the T/P ground track 107. Grey lines show where track crosses Sarykamysh lake and Large and Small Aral (dark grey — boundaries of 1962, light grey — boundaries of 18 May 2002).

(PODAAC) at the Jet Propulsion Laboratory (JPL) of California Institute of Technology (Benada, 1997; Picot et al., 2006).

The geoid field (EGM96 data) over the Aral Sea region is relatively stable (Fig. 7a). The geoid height varies from −25 to −30 m west to east for the Large Aral Sea, from −27 to −30 m in the southwestern direction for the Small Aral Sea, and from −23 to −24 m in the north-eastern direction for the Sarykamysh lake. However, the field of gravity anomalies (GA) is different (Fig. 7b). Along the T/P ground track 107, they vary from −15 to −30 mGal, what is much higher than for other parts of the sea.

In the Large Aral Sea region, the local minima of GA are located in the south-eastern shallow part (−23 mGal) and in the deep-water western part (less than −32 mGal). Along the T/P ground track 107 (Fig. 8) they do not change rapidly (−20 to −30 mGal), and GA gradient module do not exceed 0.05 mGal/km. Along the ground track 142 GA changes significantly — first GA increases from −32 to −22 mGal and then it decreases up to −23 mGal. For the Small Aral Sea, there is a minimum of below −30 mGal north of the Kokaral dam and increase of GA up to −20 to −25 mGal in the northeastern direction. The overall gradient of GA is 0.2 mGal/km along the 107 ground track.

In order to take into account all features of the GA field, the sea level is calculated in the ISADB not along the satellite ground tracks, but at crossover points or in the points equidistant from the coast. The sea level was computed for one cross-over point of the T/P (and Jason-1) tracks located in the southern part of the eastern Large Aral Sea and in one point on the track crossing the southern part of the Small Aral Sea (Fig. 1). For the Large Aral Sea, crossover point 107–142 was taken. For the Small Aral Sea, the crossover point 107–218 is too close to the cost to be safely used for the correct analysis, thus we used data in a point at 107 ascending pass, which is equidistant from the coastline.

3.2. Sea level variability

3.2.1. Large Aral Sea

Satellite data show a continuous decrease of the Large Aral Sea level modulated by seasonal and interannual signals (Fig. 9). Since 1992 and until the spring of 1995 sea level was relatively stable, then there was a rapid decrease of the sea level till summer 2002, with the rates of the sea level drop reaching 95 cm/year, on average. From October 1992 to August 2002, the water level decreased by about 6.5 m (Fig. 9). During the last years sea level drop continues, but with a much lower rate of 13.5 cm/year, on average.

Comparison of various sources of altimetric data shows that Hydroweb and USDA RDB time series correspond well with each other. The USDA RDB data are provided unsmoothed and for every cycle, thus they have more inherent noise and, in some cases, do not always correspond to the Hydroweb values due to outliers. Starting from 2003, USDA RDB data are constantly higher than Hydroweb, apparently due to different constant introduced to account for the bias between Jason-1 and T/P. ISADB monthly data in general agree well with the other time series, except for summers 1998–2000, where outliers for specific cycles could have driven the monthly values down. Apparently for the same reason as discussed for USDA RDB, the Jason-1 data from ISADB show discrepancy from Hydroweb, but this time to a smaller extent.

Some data obtained from direct geodesic levelling of the Large Aral Sea surface in field surveys can be found in (Zavialov et al., this issue).

3.2.2. Small Aral Sea

The level of the Small Aral Sea is affected not only by the constituents of the water balance, but also by the operation of the Kokaral dam in the Berg Strait (Aladin et al., 2005). Since the

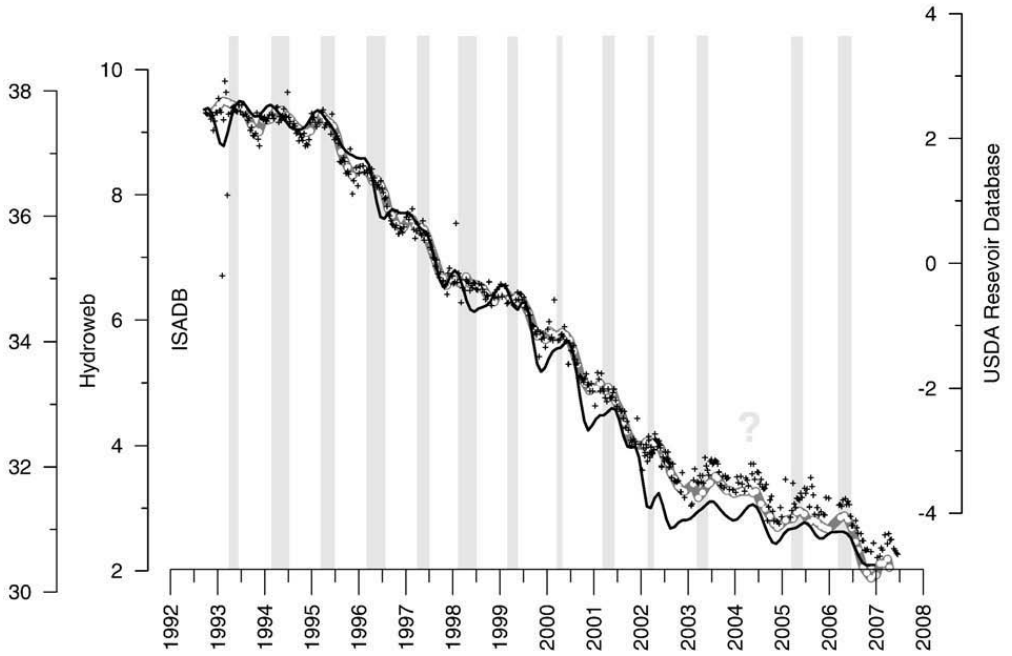

Fig. 9. Time series of Large Aral sea level (m) from various sources: ISADB (black line), Hydroweb (thick grey line with white dots), and USDA Reservoir Database (black crosses). Grey vertical lines denotes ice cover duration period (derived as described in Section 2.2.1), for 2004 the duration is absent. *Y* axis have different absolute values, but vertical scale is identical; data from various sources are overlaid in order to have the best fit for T/P.

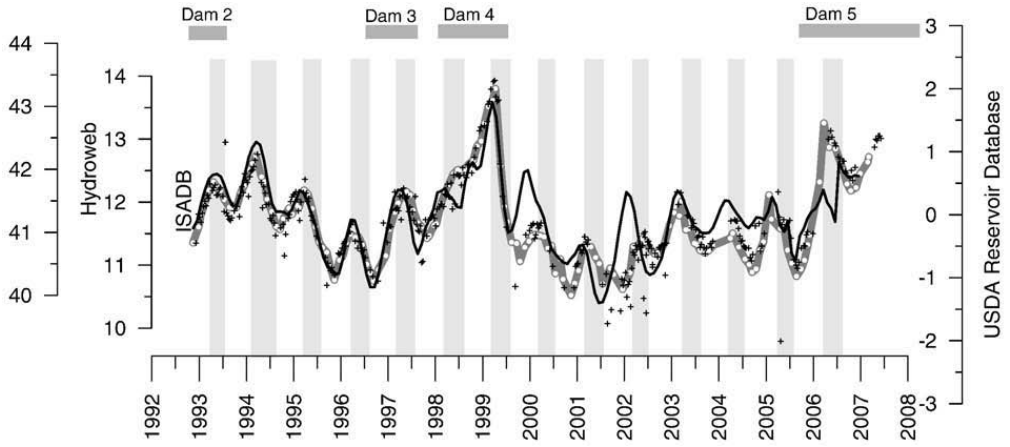

Fig. 10. Same as Fig. 9 but for Small Aral. Grey boxes in the upper part of the graph indicate the duration of Kokaral dam operations.

1980s the strait has been dredged for navigation. In the beginning of 1990s water started to flow from the northern part of the Aral Sea to the southern one; at the level of 37 m the difference between the two parts was about 3 m and the flow rate was 100 m^3/s (Aladin et al., 2005). After a separation of the Small and Big Aral in 1989, the first 1 m high sand dam was constructed in July 1992 but soon collapsed under pressure of water. Second dam of 2 m height was immediately constructed in late July – early August 1992 and stayed for 9 months until April 1993. After three years without dam a third one was constructed and operated for more than one year (April 1996 – May 1997). All three first dams have been made of sand and were not able to resist the pressure for a long time. Afterwards, a fourth, more solid (sand and concrete) dam was constructed in October 1997. This was a 14-km long and 30 m wide dam (Létolle and Chesterikoff, 1999) that stayed until 22 April 1999, when a strong storm raced through all the territory of Kazakhstan and the combined effect of waves and winter ice led once more to the dam's break-up. Before this event the Small Aral sea level was about 42.8 m. By September 1999 the sea level decreased by 2.5 m (Fig. 10). However, all the water that started to flow through the Berg Strait evaporated in the sands and did not finally reach the Big Aral (Crétaux et al., 2005). In 2003–2005 the more solid was built by the Russian company Zarubezhvodstroy under financial support of the World Bank. This fifth dam was put in operation on August 2005. These efforts resulted in a steady increase of the Small Aral Sea level since that time.

As well as those for the Large Aral Sea, the Hydroweb and USDA RDB time series for the Small Aral Sea correspond well with each other. For the Small Aral Sea, there are fewer outliers in USDA RDB than for the Large Aral Sea. Starting from 1999, these data have more gaps than Hydroweb data, probably due to filtering. For 1992–1998, ISADB data agree well with both other time series, but starting from 1999 data show much larger discrepancies, apparently affected by outliers, especially in the winter.

3.2.3. Lake Sarykamysh

Since 1992, the Sarykamysh Lake has been progressively increasing in size, reaching its maximum level at the beginning of 2000 with an increase of 5 m at a rate of 0.6 m/year, as it was observed since the beginning of the TOPEX/Poseidon altimetry mission (Fig. 11). In the next two years, a decrease of about 1 m in the lake level was observed. Since the end of 2002, we observe a continuous increase of the lake level with a rate of up to 0.7 m/year. By December 2006, Lake Sarykamysh reached its uppermost level, which was 1 m higher than in 2000. The data from both ISADB and Hydroweb reveal a similar variability, and discrepancies are rather small.

The time series of the water level for the Aral Sea and Sarykamysh Lake from the four considered data sources exhibit different data quality. For ESA river and lake, the target points are often located on land or too close to the current position of the coastline. For the points that are over the water, the time series are too short to be used for our study.

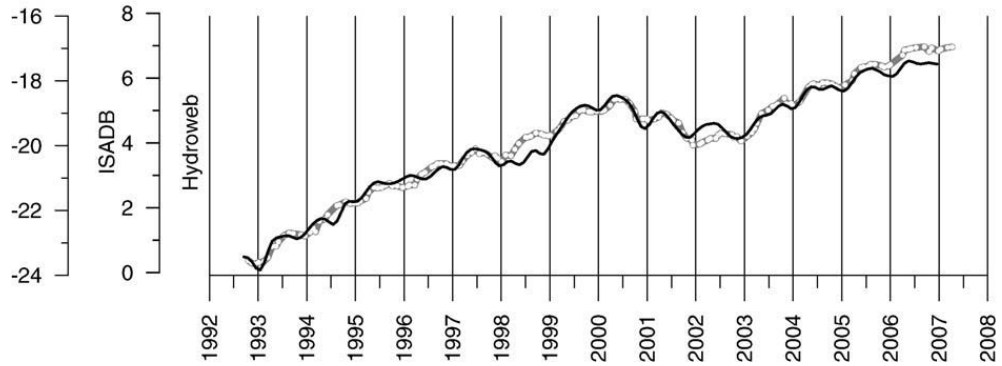

Fig. 11. Time series of Lake Sarykamysh level (m) from ISADB (black line) and Hydroweb (thick grey line with white dots). Y axis have different absolute values, but vertical scale is identical; data from various sources are overlaid in order to have the best fit for T/P.

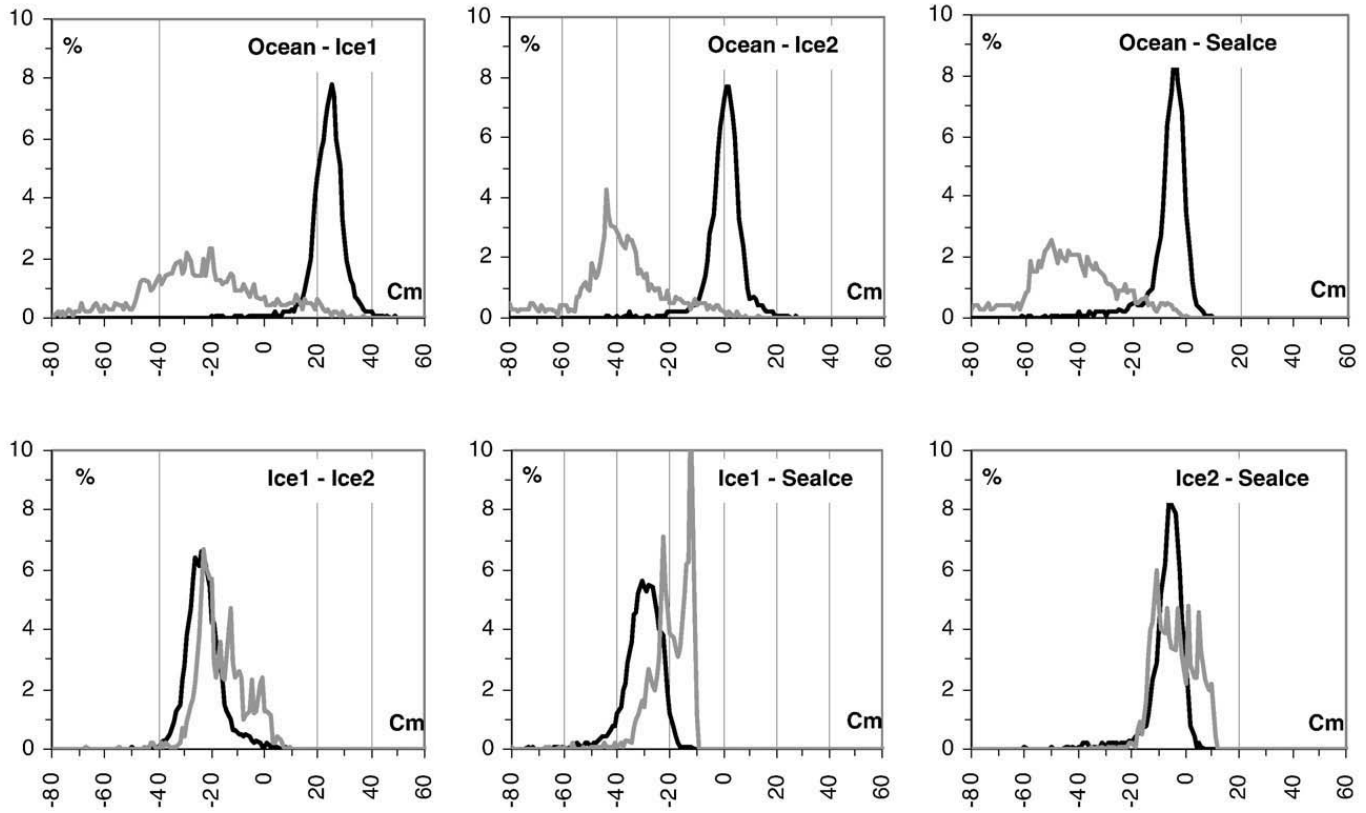

Fig. 12. Histograms (in %) of differences (cm) between 18 Hz range measures for various ENVISAT retrackers. Black lines — open water, grey lines — ice.

The Hydroweb and USDA RDB time series demonstrate the highest quality and, in general, are well correlated between each other. ISADB time series often correspond well to the other time series, but there are cases where the monthly values are strongly affected by outliers. As a result, ISADB data do not perform better than Hydroweb or USDA RDB.

3.3. Influence of sea ice on altimetric measurements

Estimates of the distance between the satellite and the echoing surface are obtained using a procedure known as altimeter waveform retracking. Retracking retrieves the point of the radar echo that corresponds to the effective satellite-to-ground range. As the primary goal of most altimeters is the study of ocean topography, most of the retracking algorithms used are suited to the open ocean conditions. For example, T/P, Jason-1, and GFO all have only one on-board retracker that is adapted to the ocean surface. However, as we have seen before, both Small and Large Aral Seas have a persistent ice cover present every year for several months. This significantly affects the shape of the returning radar waveform and could result in erroneous range estimates in winter.

In order to assess the degree to which the ice affects altimeter range measures and estimate corresponding uncertainties, we used the data from the ENVISAT altimeter. For this satellite, four different retracking algorithms (one – Ocean – for ocean conditions and three – Ice1, Ice2 and Sea Ice – for ice) were used to process the raw RA-2 radar altimeter data. The Ocean retracker uses the classical waveform shape of (Brown, 1977) and performs a fit to the measured waveform with a return power model (ESA, 2002). The Ice1 retracker has been developed for studies of both ice caps and land surfaces. This algorithm is based on the Offset Centre of Gravity (OCOG) approach (Wingham et al., 1986; Bamber, 1994). The Ice2 retracker, designed for ice caps, detects the waveform edge and fits separately an error function to the leading edge and an exponential decrease to the trailing edge (Legrésy, 1995; Legrésy and Rémy, 1997). As for sea ice there is no waveform model, the Sea Ice retracker uses a threshold approach (Laxon, 1994; ESA, 2002). For a detailed description of the four retrackers see (ESA, 2002) and for their applicability to continental water objects see (Frappart et al., 2006).

Presence of the four simultaneous range values from these retrackers for each 18 Hz RA-2 measure gives a possibility to precisely quantify the differences between various retrackers. We used the ENVISAT data for ground tracks 126, 167 and 625 for the Small Aral Sea and 253 and 670 for the Large Aral Sea

Table 1
Statistics for differences (cm) between 18 Hz range measures for various ENVISAT retrackers

	Ocean-Ice1	Ocean-Ice2	Ocean-Sea Ice	Ice1-Ice2	Ice1-SeaIce	Ice2-SeaIce
Open water						
1st quartile	20.9	−2.7	−10.6	−27.5	−36.5	−10
Median	24.9	1.4	−5.3	−23.4	−30.5	−5.8
3rd quartile	28.5	4.9	−2.2	−18.9	−25.9	−2.7
Ice cover						
1st quartile	−40.7	−52.6	−57.8	−22.9	−24.9	−10.1
Median	−25.2	−40.8	−45.6	−18.6	−19.5	−4
3rd quartile	−8.7	−30.8	−32.8	−10.3	−13.2	2.9

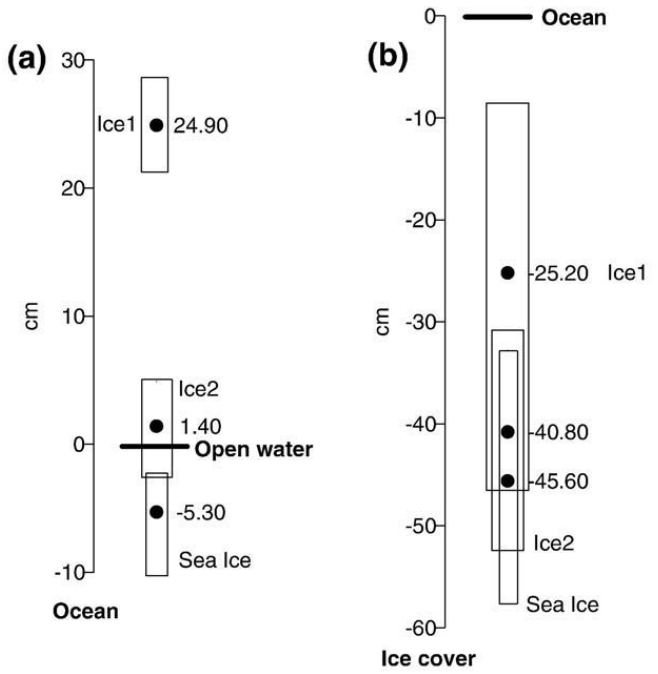

Fig. 13. Position of sea level (cm, based on values from Table 1) for Ice1, Ice2 and Sea Ice retrackers relative to Ocean retracker for open water (a) and ice cover (b). Black points — median values, lower and upper limits of boxes correspond to 1st and 3rd quartiles.

(see Fig. 4, solid black lines). Using the method described in Section 2.2.1, each 18 Hz data has been classed as either open water or ice. The total number of 18 Hz observations (each comprising four different range values from four retrackers) for open water was 11487, and that for ice was 3891. Using this dataset, we have calculated the range differences between the specific retrackers and calculated separate statistics for open water and ice (Fig. 12, Table 1).

These statistics show large variability between open water and ice cover for range differences estimated by the Ocean retracker and the three others. Median values of the ice-water differences for the corresponding retrackers amounted to 50 cm for Ocean-Ice1, 42 cm for Ocean-Ice2, and 40 cm for Ocean-Sea Ice. For these combinations of the retrackers, the shape of the histogram is narrow and high-peaked for the open water, and becomes more spread and noisy for the ice cover, reflecting high variability of the returning waveforms. The intercomparison of Ice1, Ice2 and Sea Ice retrackers initially designed to be able to process specific complex waveforms coming from ice shows much smaller differences between the open water and ice, namely, 4.8 cm for Ice1–Ice2, 11 cm for Ice1–Sea Ice, and just 1.8 cm for Ice2–Sea Ice.

Graphical representation of the sea level position as measured by the Ice1, Ice2 and Sea ice retrackers compared to the Ocean retracker is shown in Fig. 13. Though the lack of in situ measures of Aral Sea level makes it impossible to quantitatively validate these measures, we can make the comparison assuming that a) the Ocean retracker should work well for the open water, and b) the ice retrackers should work well for ice. For open water (left panel) Ocean, Ice2 and Sea Ice show similar values, while Ice1, due to retracking procedures, constantly overestimates the sea level for about 25 cm, and this should be taken into account when using Ice1 range values for the open water case.

When the lakes are ice-covered, the Sea Ice and Ice 2 values are close to each other. The Ice1 yields higher sea level height for 15–20 cm. However, the Ocean retracker constantly shows much higher values than any ice-adapted retracker, with the misfit up to 40–45 cm. We note, as an example, that for the ice-covered Ob' River in Siberia, a comparison of T/P water level and in situ observations at a closest hydrological point showed that for such a complex terrains with the influence of land and river ice, T/P underestimated the level for up to 2–3 m (!) (Kouraev et al., 2004c).

Thus, for ENVISAT, it is obviously better to use other retrackers than Ocean when the ice cover is present. For the Aral Sea, we are not able to estimate the absolute differences for each altimetric satellite, but it looks reasonable to adjust the lake level measures obtained from T/P, Jason-1, and GFO (all of which use the Ocean retracker) by additionally "lowering" them for 40–45 cm.

4. Conclusions

We discussed the recent seasonal and interannual variations of ice cover and lake surface level in the Aral Sea obtained from satellite altimetry data for the period from 1992 through 2006. An ice discrimination method, based on a synergy of active and passive data from the four altimetric missions and SSM/I, was applied to the entire satellite dataset to define specific dates of the ice events. For the Small Aral Sea, the "winter duration" (defined as the ice cover period) was stable at around 140 days, while for the Large Aral Sea this value decreased from 112 days in 1992–1997 to 69 days for 1998–2006, on average, mainly due to earlier melting of the ice. Such a rapid shortening of winter ice cover in the eastern Large Aral could be attributed to the following factors: shallowing of the sea, change of heat storage capacity, increase of salinity, decrease of the freezing temperature, lowering of temperature of maximal density, and development of thinner ice cover. In the future we plan to perform an analysis of the obtained series of ice conditions in the context of changes of both natural conditions and air temperature.

We analysed the evolution of the lake level to follow the desiccation of the Large Aral Sea, recovery of the Small Aral Sea, and filling of the Lake Sarykamysh. To this end, we used altimetric time series from several sources (Hydroweb, USDA Reservoir Database, Integrated Satellite Altimetry Data Base, and others), and performed an intercomparison of available observations. The time series of the water level for the Aral Sea and Sarykamysh Lake derived from the four considered sources showed different data quality. For ESA River and Lake, the majority of target points are mislocated, and for other points either time series are too short or the results are unrealistic. The Hydroweb and USDA RDB time series demonstrated the highest quality, and were, in general, well correlated with each other. The ISADB time series also correspond well to the above time series, but there are cases where the monthly values are strongly affected by outliers, and as a result, the ISADB data do not perform significantly better than those Hydroweb or USDA RDB.

The altimetry data show a continuous decrease of the Large Aral Sea level, modulated by seasonal and interannual signals. Since the spring of 1995, a fast decrease of the sea level was observed until the summer of 2002, with the rates

of the sea level drop reaching 95 cm/year, on average. The level drop then continued at a smaller rate of 13.5 cm/year. Using a reference point directly measured in-situ during the sea expedition in November 2002 we can reconstruct the absolute value of the sea level on 9 January 2007 that was equal to 29.42 m. This is the most recent measurement made by Jason-1 at the time of preparation of this paper.

The level of the Small Aral Sea has been largely affected by operations of the Kokaral dam. After a severe storm of 22 April 1999 that destroyed the dam, by September 1999 the sea level decreased by 2.5 m due to a continuous sink of sea water towards the Large Aral Sea. In August 2005, a new solid dam was built and this resulted in steady and rapid increase of sea level since September 2005 at the rate of 92.4 cm/year, leading to a significant recovery of the Small Aral Sea.

The Sarykamysh Lake has been progressively increasing in size since 1992, reaching its maximum level at the beginning of 2000. In the next two years, a decrease of about 1 m in the lake level was observed. Since the end of 2002, the lake experienced a continuous increase of the lake level at a rate of up to 0.7 m/year. By December 2006, the Sarykamysh Lake attained its uppermost level, which is about 1 m higher than that of 2000.

Using the data from 4 altimetric retrackers for ENVISAT, we estimated how the presence of ice could affect the altimeter range measures. We showed that for the ice-covered sea, Ocean retracker constantly yields much higher levels values than those derived from any of the ice-adapted retrackers, with the differences reaching 40–45 cm. Thus, for ENVISAT, it is obviously better to use other retrackers than Ocean when the ice cover is present. In order to homogenise the sea level time series for the open water and ice-covered sea, we suggest to subtract 40–45 cm from sea level measures from T/P, Jason-1, and GFO (all of which use the Ocean retracker) when the Aral Sea is ice-covered.

Acknowledgements

We thank Jean-François Crétaux and Benoît Legrésy (LEGOS, Toulouse, France), as well as two anonymous reviewers for the time and attention dedicated to the manuscript and for their helpful and constructive remarks. The research was supported by the NATO CLG Grant “Physical and Chemical Fluxes in Dying Aral Sea”, by the INTAS Project “ALTICORE” (Contract Nr 05-1000008-7927) and by the INTAS Project 00-1053. We are grateful to the Centre of Topographic studies of the Oceans and Hydrosphere (CTOH) at LEGOS, Toulouse, France, for supplying us with the altimetry data. This study is a contribution to the NATO collaborative linkage grant EST.CLG.980445.

References

Aladin, N., Crétaux, J.F., Plotnikov, I.S., Kouraev, A.V., Smurov, A.O., Cazenave, A., Egorov, A.N., Papa, F., 2005. Modern hydro-biological state of the Small Aral Sea. Environmetrics 16 (4), 375–392. doi:10.1002/env.709.

Armstrong, R.L., Knowles, K.W., Brodzik, M.J., Hardman, M.A., 2003. DMSP SSM/I Pathfinder daily EASE-grid brightness temperatures. National Snow and Ice Data Center Digital media and CD-ROM, Boulder, CO.

Bamber, J.L., 1994. Ice sheet altimeter processing scheme. International Journal of Remote Sensing 15 (4), 925–938.

Benada, R.J., 1997. Merged GDR (Topex/Poseidon) Generation B Users Handbook. Version 2.0. Physical Oceanography Distributed Active Archive Center (PODAAC), Jet Propulsion Laboratory, Pasadena. JPL D-11007, 131 pp.

Birkett, C.M., 1995. The contribution of Topex/Poseidon to the global monitoring of climatically sensitive lakes. Journal of Geophysical Research 100 ((C12), 25179–25204.

Birkett, C.M., 1998. Contribution of the TOPEX NASA radar altimeter to the global monitoring of large rivers and wetlands. Water Resources Research V.34 (5), 1223–1239.

Bortnik, V.N., Chistyayeva, S.P. (Eds.), 1990. Gidrometeorologiya i gidrohimiya morey. (Hydrometeorology and hydrochemistry of seas.) Vol. VII: Aral Sea. Gidrometeoizdat, Leningrad (in Russian).

Brown, G.S., 1977. The average impulse response of a rough surface and is applications. IEEE Transactions on Antennas and Propagation 25 (1), 67–74.

Cazenave, A., Bonnefond, P., Dominh, K., Schaeffer, P., 1997. Caspian sea level from Topex/Poseidon altimetry: level now falling. Geophysical Research Letters 24 (8), 881–884.

Comiso, J.C., 1986. Characteristics of Arctic winter sea ice from satellite multispectral microwave observations. Journal of Geophysical Research 91, 975–994.

Crétaux, J.F., Birkett, C., 2006. Lake studies from satellite altimetry. C R Geoscience 338 (14–15), 1098–1112. doi:10.1016/J.cre.2006.08.002 (November–December 2006).

Crétaux, J.F., Kouraev, A.V., Papa, F., Bergé-Nguyen, V., Cazenave, A., Aladin, N., Plotnikov, I.S., 2005. Water balance of the Big Aral Sea from satellite remote sensing and in situ observations. Journal of Great Lakes Research 31 (4), 520–534.

ESA, 2002. ENVISAT RA2/MWR Product Handbook, RA2/MWR Products User Guide ESA.

ESA River and Lakes web site (accessed June 2007): http://earth.esa.int/riverandlake/.

Frappart, F., Calmant, S., Cauhopé, M., Seyler, F., et al., 2006. Cazenave, results of ENVISAT RA-2 derived levels validation over the Amazon basin. Remote Sensing of Environment 100, 252–264.

Ginzburg, A.I., Kostianoy, A.G., Sheremet, N.A., 2003. Thermal regime of the Aral Sea in the modern period (1982–2000) as revealed by satellite data. Journal of Marine Systems 43, 19–30.

Glantz, M.H. (Ed.), 1999. Creeping Environmental Problems and Sustainable Development in the Aral Sea Basin. Cambridge University Press. 304 pp.

Glazovsky, N.F., 1995a. Aral Sea. In: Mandych, A.F. (Ed.), Enclosed Seas and Large Lakes of Eastern Europe and Middle Asia. SPB Academic Publishing, Amsterdam, The Netherlands, pp. 119–154.

Glazovsky, N.F., 1995b. The Aral Sea Basin. In: Kasperson, Jeanne X., Kasperson, Roger E., TurnerII II, B.L. (Eds.), Regions at Risk: Comparisons of Threatened Environments. United Nations University Press, Tokyo.

Hydroweb web site (accessed June 2007): http://www.legos.obs-mip.fr/soa/hydrologie/hydroweb/.

Koblinsky, C.J., Ray, R., Becley, B.D., et al., 1999. NASA Ocean Altimeter Pathfinder Project. NASA Goddard Space Flight Center. — Report 1: Data Processing Handbook, NASA/TM-1998-208605, 55 pp. — Report 2: Data Set Validation, NASA/TM-1999-209230. 56 pp.

Kosarev, A.N., 1975. Gidrologiya Kaspiyskogo i Aral'skogo morey (Hydrology of the Caspian and Aral seas). Moscow University Publishing. 271 pp. (in Russian).

Kostianoy, A.G., 2006. Dead and dying seas. Encyclopedia of Water Science. Taylor & Francis. doi:10.1081/E-EWS-120042068.

Kostianoy, A.G., Wiseman, W. (Eds.), 2004. The Dying Aral Sea. Special Issue of J. Marine Systems. 2004. V.47(1–4). 152 pp.

Kostianoy, A.G., Zavialov, P.O., Lebedev, S.A., 2004. What do we know about dead, dying and endangered lakes and seas? In: Nihoul, J.C.J., Zavialov, P.O., Micklin, Ph.P. (Eds.), Dying and Dead Seas. Climatic versus Anthropic Causes. Kluwer Acad. Publ., Dordrecht, pp. 1–48. NATO ARW/ASI Series.

Kostianoy, Andrey G., Kosarev, Aleksey N. (Eds.), 2005. The Caspian Sea Environment. Series : The Handbook of Environmental Chemistry, Vol. 5 : Water Pollution , Part 5P. ISBN: 978-3-540-28281-5. XIV, 271 pp.

Kouraev, A.V., Papa, F., Buharizin, P.I., Cazenave, A., Crétaux, J.-F., Dozortseva, J., Remy, F., 2003. Ice cover variability in the Caspian and Aral seas from active and passive satellite microwave data. Polar Research 22 (1), 43–50.

Kouraev, A.V., Papa, F., Mognard, N.M., Buharizin, P.I., Cazenave, A., Crétaux, J.F., Dozortseva, J., Remy, F., 2004a. Sea ice cover in the Caspian and Aral seas from historical and satellite data. Journal of Marine Systems 47, 89–100.

Kouraev, A.V., Papa, F., Mognard, N.M., Buharizin, P.I., Cazenave, A., Crétaux, J.F., Dozortseva, J., Remy, F., 2004b. Synergy of active and passive satellite microwave data for the study of first-year sea ice in the Caspian and Aral seas. IEEE Transactions on Geoscience and Remote Sensing (TGARS) 42 (10), 2170–2176 October 2004.

Kouraev, A.V., Zakharova, E.A., Samain, O., Mognard-Campbell, N., Cazenave, A., 2004c. Ob' river discharge from TOPEX/Poseidon satellite altimetry data. Remote Sensing of Environment 93, 238–245.

Kouraev, A.V., Semovski, S.V., Shimaraev, M.N., Mognard, N.M., Legresy, B., Remy, F., 2007a. Observations of lake Baikal ice from satellite altimetry and radiometry. Remote Sensing of Environment 108 (3), 240–253.

Kouraev, A.V., Semovski, S.V., Shimaraev, M.N., Mognard, N.M., Legresy, B., Remy, F., 2007b. Ice regime of lake Baikal from historical and satellite data: Influence of thermal and dynamic factors. Limnology and Oceanography 52 (3), 1268–1286.

Larnicol, G., Le Traon, P.-Y., Ayoub, N., De Mey, P., 1995. Mean sea level and surface circulation variability of the Mediterranean Sea from 2 years of TOPEX/POSEIDON altimetry. Journal of Geophysical Research 100 (C12), 25163–25177.

Laxon, S., 1994. Sea ice altimeter processing scheme at the EODC. International Journal of Remote Sensing 15 (4), 915–924.

Lebedev, S.A., Kostianoy, A.G., 2005. Satellite Altimetry of the Caspian Sea. Sea, Moscow. 366 pp. (in Russian).

Legrésy, B., 1995. Etude du retracking des surfaces des formes d'onde altimétriques au-dessus des calottes, rapport CNES, CT/ED/TU/UD96.188, contrat no 856/2/95/CNES/006. 81 pp.

Legrésy, B., Rémy, F., 1997. Surface characteristics of the Antarctic ice sheet and altimetric observations. Journal of Glaciology 43 (144), 197–206.

Létolle, R., Chesterikoff, A., 1999. Salinity of surface waters in the Aral sea region. International Journal of Salt Lake Research 8 (4), 293–306. doi:10.1007/BF02442116.

Létolle, R., Mainguet, M., 1993. Aral. Springer Verlag, Paris. 357 pp.

Medvedev, P.P., Lebedev, S.A., Tyupkin, Y.S., 1997. An integrated data base of altimetric satellite for Fundamental geosciences research. Proc. First East-European Symp. Advances in Data Bases and Information Systems (ADBIS'97) St.-Petersburg, Russia, September 2-5, 1997, vol. 2. St.-Petersburg University, St.-Petersburg, pp. 95–96.

Mercier, F., 2001. Altimétrie spatiale sur les eaux continentales: apport des missions TOPEX/POSEIDON et ERS-1&2 à l'étude des lacs, mers intérieures et bassins fluviaux. Thèse de doctorat de l'Université Paul Sabatier, Toulouse, 240 pp.

Mercier, F., Cazenave, A., 2001. Lake level fluctuations in Eastern Europe and Asia from Topex/Poseidon data. EGS XXVI General Assembly, Nice, France.

Mercier, F., Cazenave, A., Maheu, C., 2002. Interannual lake level fluctuations in Africa (1993–1999) from Topex-Poseidon: connections with ocean-atmosphere interactions over the Indian Ocean. Global and Planetary Change 32, 141–163.

Micklin, P.P., 1988. Dessication of the Aral Sea: a water management disaster in the Soviet Union. Science 241, 1170–1176.

Micklin, P.P., Williams, W.D. (Eds.), 1996. The Aral Sea Basin NATO ASI Series (Partnership Sub-series, Environment, 12. Springer-Verlag. 186 pp. (Proc. NATO Advanced Research Workshop, Tashkent, Uzbekistan, 1994.).

Mikhailov, V.N., Kravtsova, V.I., Gurov, F.N., Markov, D.V., Gregoire, M., 2001. Assessment of the present-day state of the Aral Sea. Vestnik Moskovskogo Universiteta, Geographic Series 6, 14–21 in Russian.

Mirabdullayev, I.M., Joldasova, I.M., Mustafaeva, Z.A., Kazakhbaev, S., Lyubimova, S.A., Tashmukhamedov, B.A., 2004. Succession of the ecosystems of the Aral Sea during its transition from oligohaline to polyhaline water body. Journal of Marine Systems 47, 101–107.

Morris, G.S., Gill, S.K., 1994a. Variation of Great Lakes water levels derived from GEOSAT altimetry. Water Resources Research 30 (4), 1009–1017.

Morris, G.S., Gill, S.K., 1994b. Evaluation of the Topex/Poseidon altimeter system over the Great Lakes. Journal of Geophysical Research 99 (C12), 24527–24540.

Nezlin, N.P., Kostianoy, A.G., Li, B.L., 2005. Interannual variability and interaction of remote-sensed vegetation and atmospheric precipitation in the Aral Sea Region. Journal of Arid Environments 62 (4), 677–700.

Nihoul, J.C.J., Kosarev, A.N., Kostianoy, A.G., Zonn, I.S. (Eds.), 2002. The Aral Sea: Selected Bibliography. Noosphere, Moscow. 232 pp.

Peneva, E.L., Stanev, E.V., Stanychni, S.V., et al., 2004. The recent evolution of the Aral Sea level and water properties: analysis of satellite, gauge and hydro-meteorological data. J. Mar. Syst. 47, 11–24.

Picot, N., Case, K., Desai, S., Vincent, P. (2006), AVISO and PODAAC User Handbook. IGDR and GDR Jason Products. SMMMUM5OP13184CN (AVISO). JPL D21352 (PODAAC), Edition 3.0, 115 pp.

Stanev, E.V., Peneva, E.L., Mercier, F., 2004. temporal and spatial patterns of sea level in inland basins: recent events in the Aral Sea. Geophysical Research Letters 31, L15505. doi:10.1029/2004GL020478.

Steffen, K., Key, J., Cavalieri, D.J., Comiso, J., Gloersen, P., St.Germain, K., Rubinstein, I., 1992. The estimation of geophysical parameters using passive microwave algorithms. In: Carsey, F.D. (Ed.), Microwave Remote Sensing of Sea Ice. AGU: Geophysical Monograph, vol. 68.

Swift, C.T., Cavalieri, D.J., 1985. Passive microwave remote sensing for sea ice research. EOS 66 (49), 1210–1212.

Ulaby, F.T., Moore, R.K., Fung, A.K., 1986. Microwave remote sensing, Active and Passive, Vol. III, From theory to applications. Artech House, Inc.

USDA Reservoir Database web site (accessed June 2007): http://www.pecad.fas.usda.gov/cropexplorer/global_reservoir/.

Wingham, D.J., Rapley, C.G., Griffiths, H., 1986. New techniques in satellite altimeter tracking systems. Proceedings of IGARSS'8'6 Symposium, Zurich, 8 –11 Sept. 1986, Ref. ESA SP-254, pp. 1339–1344.

Zavialov, P.O., 2005. Physical Oceanography of the Dying Aral Sea. Springer Praxis Books. 146 pp.

Zavialov, P.O., Kostianoy, A.G., Emelianov, S.V., Ni, A.A., Ishniyazov, D., Khan, V.M., Kudyshkin, T.V., 2003a. Hydrographic survey in the dying Aral Sea. Geophysical Research Letters 30, 1659–1662. doi:10.1029/2003GL017427.

Zavialov, P.O., Kostianoy, A.G., Sapozhnikov, Ph.V., Scheglov, M.A., Khan, V.M., Ni, A.A., Kudyshkin, T.V., Pinkhasov, B.I., Ishniyazov, D.P., Petrov, M.A., Kurbaniyazov, A.K., Abdullaev, U.R., 2003b. Modern hydrophysical and hydrobiological state of the western Aral Sea. Okeanologiya 43 (2), 316–319 (in Russian).

Zonn, I.S., Glantz, M., 2008. The Aral Sea Encyclopedia. Kosarev, A.N., Kostianoy, A.G. (Eds.), Mezhdunarodnye Otnosheniya, Moscow (in Russian), 256 pp.

Annex 2. Reconstructing river discharge from altimetric water level measures and in situ data (Ob' river)

Kouraev A.V., Zakharova E.A., Samain O., Mognard-Campbell N., Cazenave A. "Ob' river discharge from TOPEX/Poseidon satellite altimetry data", Remote Sensing of Environment, 93, 2004, pp. 238-24

Available online at www.sciencedirect.com
SCIENCE DIRECT
Remote Sensing of Environment 93 (2004) 238–245
Remote Sensing of Environment
www.elsevier.com/locate/rse

Ob' river discharge from TOPEX/Poseidon satellite altimetry (1992–2002)

Alexei V. Kouraev[a,b,*], Elena A. Zakharova[b], Olivier Samain[c], Nelly M. Mognard[a], Anny Cazenave[a]

[a]*Laboratoire d'Etudes en Géophysique et Océanographie Spatiales (LEGOS), Toulouse, France*
[b]*State Oceanography Institute, St. Petersburg Branch, St. Petersburg, Russia*
[c]*Météo-France, CNRM, Toulouse, France*

Received 14 January 2004; received in revised form 7 July 2004; accepted 11 July 2004

Abstract

The paper discusses an application of the TOPEX/Poseidon (T/P) altimetry data to estimate the discharge of one of the largest Arctic rivers—the Ob' river. We first discuss the methodology to select and retrieve the altimeter water levels during the various phases of the hydrological regime. Then we establish the relationships between the satellite-derived water levels and the in situ river discharge measurements at the Salekhard gauging station near the Ob' estuary. The comparison of in situ and satellite-derived estimations of the Ob' discharge at Salekhard shows that the T/P data can successfully be used for hydrological studies of this river. We address the problems affecting the accuracy of the discharge estimations from altimeter measurements, identify potential solutions and suggest how satellite altimetry data may benefit hydrological studies of Arctic rivers.

Keywords: Radar altimetry; Ob' river level and discharge; TOPEX/Poseidon

1. Introduction

Rivers are an integral part of the global climate system, sensitive to its regional and global variations. and therefore a strong indicator of climate change. Global warming is expected to be the most significant with strong feedback on global climate in the arctic regions (IPCC, 2001). Climatic change will lead to potential increase in freshwater release into the Arctic Ocean, which in turn will affect thermohaline circulation, as well as ice and North Atlantic Deep Water (NADW) formation (Broecker, 1997; Rahmstorf, 1995). Peterson et al. (2002) have shown using in situ river monitoring data that the average annual discharge of freshwater from the largest Eurasian rivers to the Arctic Ocean has already increased by 7% from 1936 to 1999.

In situ measurements of river discharge are rather sparse in the remote Arctic environments. Besides this, a general decline in the arctic hydrologic monitoring network has begun in the mid-1980s (Shiklomanov et al., 2002). These conditions make microwave satellite sensor measurements an essential complement to in situ observations, and in some cases, to serve as virtual gauging stations. Recently, it has been demonstrated that TOPEX/Poseidon (T/P) altimetry could provide valuable information on water level variations of rivers, wetlands and floodplains with the precision of several tens of centimetres (Birkett, 1995, 1998; Bjerklie et al., 2003; de Olivera Campos et al., 2001; Maheu et al., 2003; Mercier, 2001).

Most of the altimeter-based studies on river streamflow have been performed in tropical or equatorial regions. Here we assess the applicability of satellite altimetry data for arctic rivers, where the presence of ice and snow perturbs the altimetric signal during a large portion of the year. One of the largest Eurasian rivers—the Ob' river—was chosen in order to estimate the accuracy of the T/P

* Corresponding author. LEGOS, 18 Avenue Edouard Belin, 31401 Toulouse Cedex 9, France. Tel.: +33 561 332902.
E-mail address: akou2@mail.ru (A.V. Kouraev).

0034-4257/$ - see front matter © 2004 Elsevier Inc. All rights reserved.
doi:10.1016/j.rse.2004.07.007

altimetric measurements of river level and discharge. We first discuss the methodology used to select and retrieve the altimeter water levels during the various phases of the Ob' hydrological regime. Next, we establish relationships between satellite-derived water level and river discharge measurements at Salekhard gauging station near the Ob' estuary. We consider a simplified relation between the water level (H) and river discharge (Q) without the use of detailed in situ information on hydraulic and morphological particularities of the chosen river section. This simplification is done in order to estimate the applicability of such an approach for conditions when such base information is not available. The calculated discharges are then compared with in situ measurements and an assessment of the accuracy of the altimeter discharge estimates is performed.

2. The Ob' river and its hydrological regime

The Ob' has the largest watershed of all Arctic rivers (2,975,106 km^2) and is the third largest contributors of freshwater to the Arctic ocean (mean annual flow of 402 km^3/year) after the Yenisey and Lena rivers (Russia: river basins, 1999). The Ob' length is 3,680 km from the confluence of Biya and Katun' rivers in the Altay mountain region to the Ob' bay in the Kara sea. According to the hydrographic conditions and river regime, the Ob' is usually divided into the three main parts (Fig. 1)—the Upper Ob' (from the confluence of Biya and Katun' up to the confluence of Ob' and Tom'), the Middle Ob' (from the Tom' mouth to the Irtysh mouth), and the lower Ob' (from the Irtysh mouth to the Ob' bay). The object of our study is the lower Ob' near its confluence to the Ob' bay.

The Ob' hydrographical network is characterised by a sharp asymmetry—most of the watershed area (67% of the total area) is located on the left-bank. Another typical feature is the presence of areas of inner discharge (not providing inflow to the Ob' river system), which cover 15% of the watershed area. A large part of the watershed is located within the West Siberian plain and the flat relief significantly affects the hydrographical network. In the region of the lower Irtysh and lower Ob', there are 70,000 water streams, 89% of them being less than 10 km long (Russia: river basins, 1999). The Ob' of the West Siberian plain is also characterised by large flooded areas, frequently described as the biggest world swamp. The region is abundant with lakes (over 450,000), mainly small lakes with surface area less than 1 km^2 and depths of 2–5 m.

The distribution of the river discharge in various parts of the Ob' river system has complex patterns with long flood periods. The latitudinal extent of the Ob' watershed (from 47°N to 68°N) results in the gradual melting of snow during the spring and in a smooth temporal distribution of the discharge during the flooding period. The Ob' discharge starts to increase in April, when the flood wave begins to break the ice cover, and reaches maximal values in May–June. During this time, large areas of the Ob' basin are flooded. The discharge then gradually decreases until July–August, and in September–October an autumn low level period is observed. About 75–80% of the annual flow is observed during the open water period before the river gets covered by ice until the next spring.

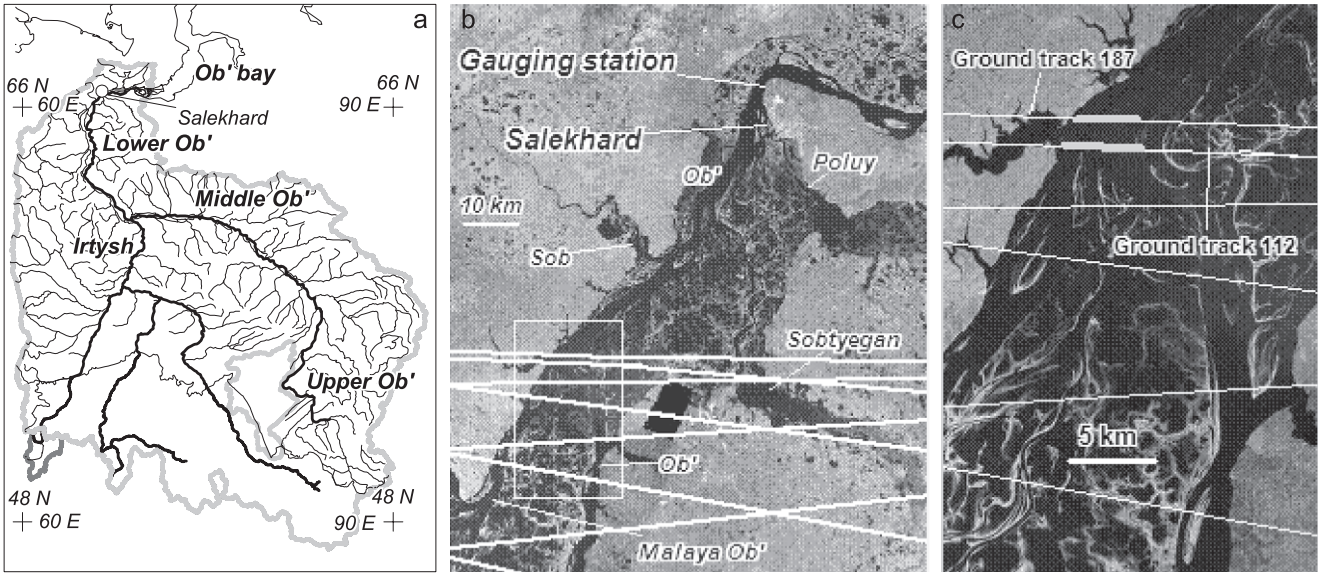

Fig. 1. (a) Ob' watershed and river network. (b) Landsat Thematic Mapper image with superimposed T/P ground tracks (white lines) near the Salekhard gauging station. (c) Zoom on the white rectangle shown in (b), thick gray lines represent the intersections of the T/P ground tracks with the main Ob' channel.

3. Data

3.1. In situ data

To establish the relations between satellite and in situ measurements, we used the river level and discharge measured at the Salekhard station (last observation point before the Ob' enters the Ob' bay and the Kara sea), one of the few gauging stations for which appropriate data is available. Mean monthly values were obtained from R-ArcticNet web site (R-ArcticNet, 2003) from 1992 to 2001 and complemented by daily river level and discharge data (R. Holmes, personal communication) after January 2000 acquired from the ArcticRIMS web site (ArcticRIMS, 2003). Additional data on daily level and discharge observations for 1970 were acquired from (State Water Cadaster, 1971).

3.2. Satellite altimetry data

A satellite radar altimeter performs vertical range measurements between the satellite and the reflecting water surface. The difference between the satellite altitude above a reference surface (either a conventional ellipsoid or a model geoid surface) determined through precise orbit computation, and the distance from the satellite to the water provides a measurement of the water level above the reference surface (altimeter range). Placed onto a repeat orbit, the satellite altimeter overflies a given region at regular time intervals (called the orbital cycle). The TOPEX/Poseidon radar altimeter is on a 10-day repeat orbit, well suited to monitor rivers discharge variations, while the 35-day repeat orbit of the ERS altimeters is too coarse especially for Arctic rivers who are subject to intense increase in discharge over 1- or 2-month periods in the spring when snow melts.

The TOPEX/Poseidon (T/P) altimetry data were obtained from the Geophysical Data Records (GDR-Ms) available from the Archiving Validation and Interpretation of Satellite Data in Oceanography (AVISO) data center at the Centre National d'Etudes Spatiales (CNES) (AVISO, 1996) and consist of range values from radar echoes at 1/10 s and averaged values at 1 s interval, corresponding to along-track ground spacing of 596 m and 5.96 km, respectively. The inclination of the T/P orbit (66°) allows for most of the Ob' basin to be sampled by numerous intersections between satellite ground tracks and rivers at a 10-day resolution (the duration of an orbital cycle). Ten years of satellite altimetry data have been analysed covering the period from September 1992 to August 2002 (cycles 1 through 365), before T/P was moved to a new orbit. Environmental and geophysical corrections of the altimeter range measurements relevant to the Ob' basin have been applied. The corrections applied include ionospheric, dry tropospheric, solid Earth tide corrections and correction for the satellite's centre of gravity. We neglect, on the other hand, corrections specific to open ocean environments such as ocean and pole tides, ocean tide loading, inverted barometer effect and sea state bias. The wet tropospheric correction, normally derived from the onboard TOPEX Microwave Radiometer (TMR) over oceans, is not available over land in the GDR-Ms. The TMR instrument has a large footprint (up to 43.4 km in diameter for the 18 GHz channel). When the satellite flies over rivers, the TMR footprint almost always includes surrounding lands, which contaminates the measurements and makes atmospheric water vapor measurement unreliable. However, over land, the wet tropospheric correction can be modelled using meteorological operational analyses and it has been computed for the whole T/P mission by Mercier (2003) using air temperature and specific humidity fields from National Centers for Environmental Predictions (NCEP) meteorological fields. The water heights have been referred to the JGM3/OSU95A geoid surface (AVISO, 1996).

4. Ob' river level and discharge from Topex/Poseidon

4.1. Data selection

A mountainous topography may lead the altimeter to lock off completely, requiring some time to lock on again; even over water and for narrow rivers the instrument may deliver no reliable measurement at all. In other cases, the instrument could remain locked on water while the satellite is well ahead of the water body, since the reflected signal on water has more power than the reflected signal on land. This may cause a geometric error that could reach several meters for some regions.

In order to minimise potential contamination of the T/P signal by land reflections, and at the same time to retain a sufficiently large number of altimeter measurements on water, we performed a geographical selection of the data. We used GeoCover™ Landsat Thematic Mapper orthorectified mosaics with 28.5 m pixel size available from the MrSID Image Server (MrSID web site, 2003) to select with a high spatial resolution the most appropriate satellite tracks–river intersections. The width of the Ob' River in this region changes seasonally from 2 to 20 km depending on the phase of the hydrological regime. To get consistent measurements in various phases of the water regime, we selected only those parts of the T/P ground tracks that cover the main channel of the Ob' river system (Fig. 1c). This rigorous selection was made using the 1/10 s level measurements.

Over continents, radar echoes are affected by topography, vegetation, ice and snow cover. As a consequence, the waveform (i.e. the power distribution in time of the radar echo) may not have the simple broad-peaked shape typical of ocean surfaces, but can be complex and multi-peaked (Berry, 2003; Birkett, 1998). The existing T/P ocean retracking algorithm is not designed to process

such signals and this affects the precision of determination of the altimetric height. For the relatively flat lower Ob' region near Salekhard, the presence of ice and snow (on land and on river ice) perturbs the altimeter measurements, which are strongly attenuated by their presence (Kouraev et al., 2003a; Papa et al., 2002). The characteristics of the radar echo over ice and snow depend on the volume scattering effect of the media and the two-way attenuation of the return signal.

Snow over land in this region is not very deep (the total annual amount of solid precipitation varies between 100 and 200 mm) (World Atlas of Snow and Ice Resources, 1997) and the precise geographic selection of the T/P data reduces the potential influence of snow-covered land on the altimetric signal. The ice cover, which is present for more than half of the year, influences significantly the radar waveform and backscatter values not only in periods of stable ice cover, but also during ice formation and break-up (Kouraev et al., 2003b). A new retracking algorithms adapted to various terrain such as open and ice-covered rivers will increase the reliability of river level estimates from altimetry observations (Berry, 2003). Until new algorithms better adapted to land become available, we use the standard GDRs that offer useful information on land waters (Birkett, 1998).

Due to the 66°N inclination of the satellite orbit, the closest satellite pass to the Salekhard station is located approximately 65 km south of the station (Fig. 1). For the lower Ob' basin, the T/P measurements along the tracks close to Salekhard provide reliable water level (H) time series that are used to estimate water discharge (Q) from the rating curve between H and Q. We used the in situ daily discharge data acquired during 2000–2002 at the Salekhard gauging station (ArcticRIMS, 2003) and the data from the two T/P ground tracks (112 and 187), nearest to Salekhard. The distance between the gauging station and these T/P tracks is about 65–70 km, while the distance between the two satellite tracks is 2.5 km. The two chosen satellite tracks sample the Ob' in the relatively narrow area just after the confluence of the two main branches of the Ob' in its lower part—Ob' and Small Ob' (see Fig. 1b). Between the satellite tracks and Salekhard, there are only three small rivers—Sob', Sob'yegan and Poluy. The largest river is Poluy with an annual discharge of 4.1 km^3/year (ArcticRIMS, 2003) representing about 1% of the Ob' discharge at Salekhard, so the influence of lateral river inflow between the chosen T/P tracks and Salekhard can be neglected for this study.

The Ob' valley near the tracks 112 and 187 has several secondary channels and vast flood plains in its eastern part. By mid-May, the plain is rapidly flooded and then the water gradually returns into the main channel, thus increasing the flood period. Numerous old channels, lakes and bogs have water level regimes that differ from the main channel. As a result, the satellite time series of water level are noisy and a precise geographical selection is necessary to establish a robust H–Q relation. To eliminate the noise, we only considered the data over the main Ob' channel, which is about 3 km wide (see Fig. 1). Next, we averaged the selected 1/10 s level measurements and constructed the T/P water level time series over the orbital cycle (10-day interval). At the beginning of the flood, the number of T/P data in the GDR-Ms dramatically drops, mostly because the onboard automatic tracker algorithm experiences difficulties in processing the return waveform significantly modified by the ice cover break-up. We consider the relation H–Q for each of the two tracks and establish an algorithm to calculate the discharge from the T/P level time series.

4.2. River level

The water levels at Salekhard and along the T/P tracks vary synchronously and the time series are dominated by the annual cycle. The superposition of the two series (Fig. 2),

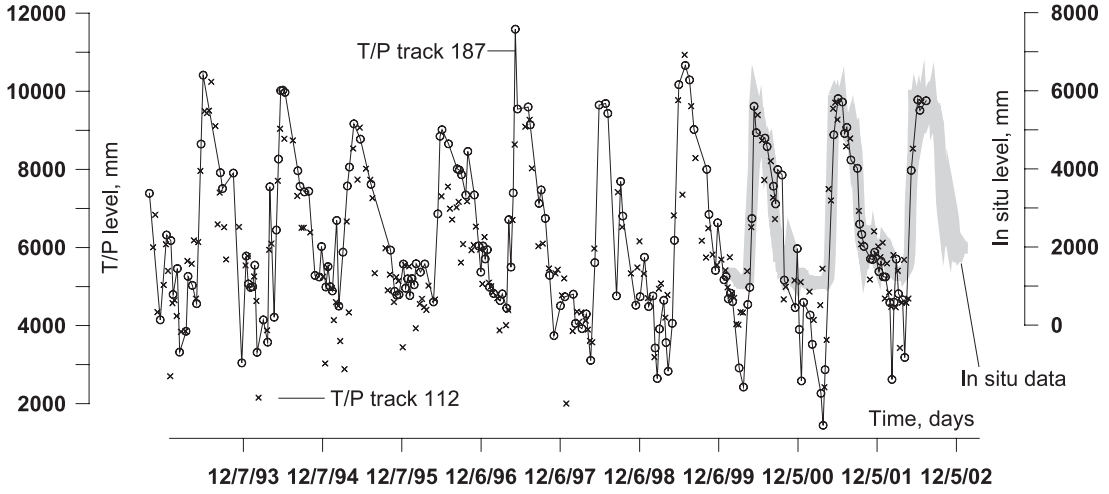

Fig. 2. Time series of T/P water level for tracks 187 and 112 (referred to the JGM3/OSU95A geoid surface), and in situ data at Salekhard (referred to the gauging station datum) overlaid on T/P data.

altimeter-derived data referred to the geoid and in situ measurements refer to gauging station datum, shows that during the open water period the timing and the amplitude of the river level variability are very close. The standard deviation of the 1/10 s level measurements available for each cycle at ground track 187 changes from 40 cm during spring flood to 23 cm during water level decrease in late summer early fall. With the presence of ice, the standard deviation increases again up to 30 cm. During winter, when the river is ice-covered, the T/P level series become unstable and have lower values (up to 2–3 m) compared to the level observed at Salekhard.

There is a time lag in river level between Salekhard and the satellite tracks and this lag varies for the different hydrological phases. As the flood wave and related ice break-up propagates northward, the beginning of the spring flood at the T/P tracks is about 20 days earlier. When the ice has gone, the flood wave moves freely and the time lag for the highest water levels is reduced to less than 5 days. In autumn, the formation of young ice often causes temporal water level increase related to the constriction of the river channel cross section. As the formation of the ice moves southward, first small peaks are observed at Salekhard, and then at the satellite tracks, with time lag of 25–30 days.

4.3. Level–discharge relation

The water discharge is functionally related to the water level at the given location. This relation, called the "stage–discharge rating curve" (or simply "rating curve") is determined from simultaneous measurements of water level and corresponding discharge and can be simple or complex. The simplest forms of the rating curves are observed in the cases of stable channels with steady flow. The rating typically follows the power law given by the equation (Ranz et al., 1982)

$$Q = C(H - e)^b$$

where Q is the discharge, H the water level, and C, e and b are coefficients. A polynomial function can be used to fit the curves. Amongst the factors controlling the ratio are the shape of the riverbed, scour of channel, rapid changes of flow (unsteady flow), changes in hydraulic roughness (seasonal development of water vegetation, debris, sediment redeposition, ice), backwater effect, etc. Usually, the stage–discharge rating for a given point consists of the whole family of curves corresponding to different periods when the flow is assumed to be steady. Very often, the simple temporal analysis of the water level and discharge series already provides the possibility to discriminate the main periods of quasi-steady flow. Further detailed studies specific for each river are directed towards assessing the main factors responsible for the unsteadiness and for adjusting the rating curves according to these factors.

For rivers with vast flood plains like the Ob', the rating curve consists of several branches corresponding to the different hydraulic conditions (or hydrological phases) (Bykov & Vasiliev, 1973). The H–Q diagram based on the daily water level and discharge in situ data for 1970 and for 2001 (Fig. 3a) shows these branches. The good relation between the data for 1970 and 2001 shows that for the last 30 years there were no significant changes in the factors that could have affect H–Q relation at the Salekhard station.

In order to reconstruct the discharge at Salekhard from the T/P data, we directly constructed the rating curves between the T/P-derived river level (H) at the satellite tracks and the river discharge at Salekhard (Q) (Fig. 3b). This

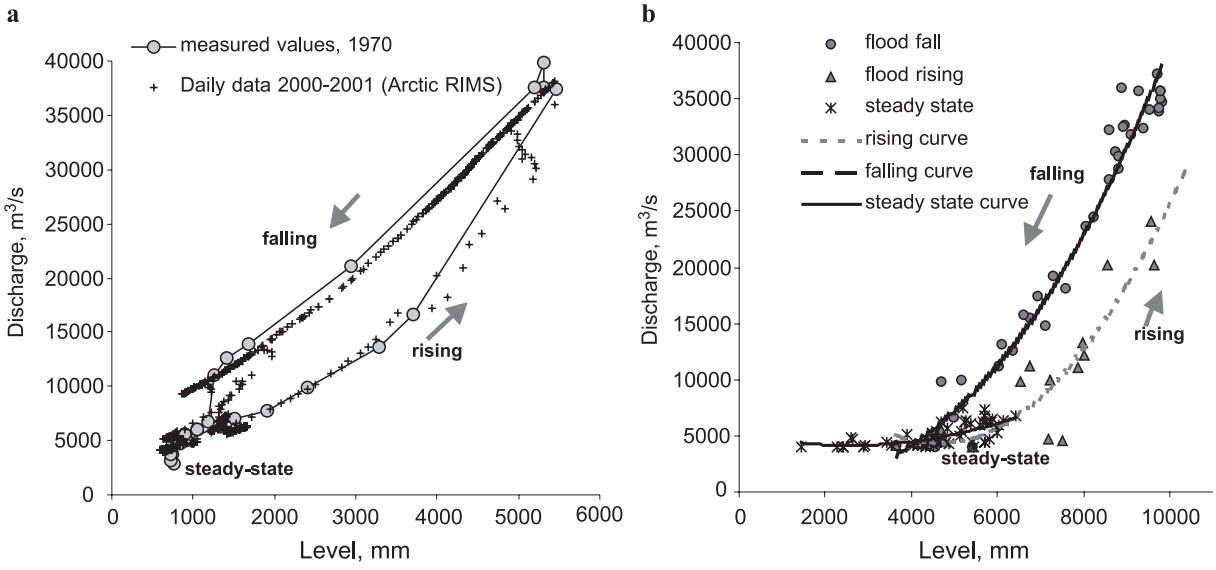

Fig. 3. H–Q relation as a function of the hydrological phases: (a) in situ data (1970 and 2001); (b) T/P data for 2000–2002.

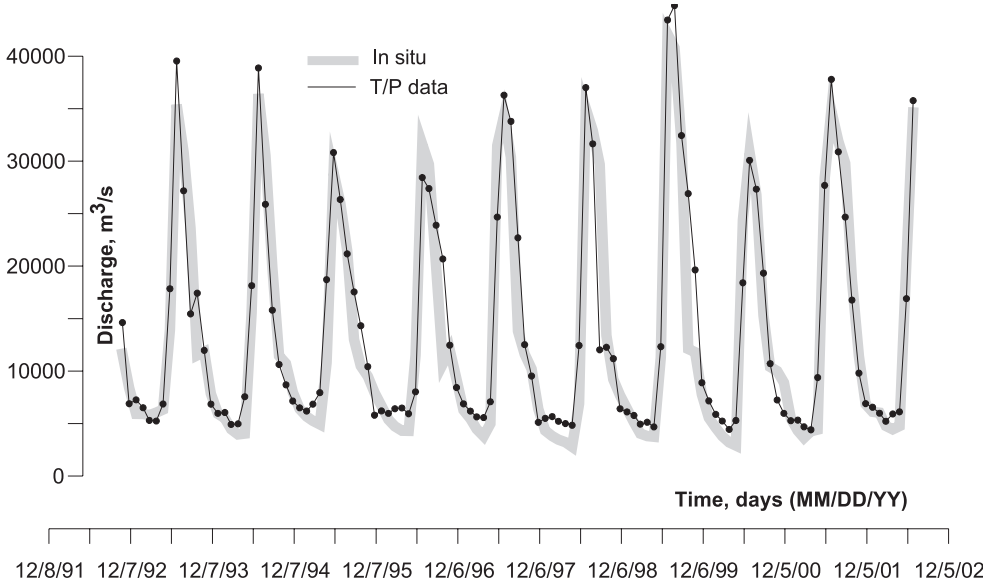

Fig. 4. Mean monthly water flow (m^3/s) at Salekhard from in situ and satellite-derived data (ground track 187).

direct calculation significantly reduces the potential errors, compared to other possible approach which consist of using the T/P-derived river level to reconstruct the river level at Salekhard and then applying the various existing rating curves for Salerkhard gauging station to calculate the discharge.

The data have been divided into three subperiods: flood rising, flood falling and a winter period of quasi-steady conditions. For 2000–2002 when we have access to daily discharge data, we have constructed the diagrams $Q=f(H_{T/P})$ and approximated the points for each of the three periods by polynomial functions (Fig. 3b). Then, we have calculated Q for each T/P crossing for 1992–2002 and interpolated the data to calculate the Q values for every day of the year in order to compute monthly Q values and compare them to the RIMS data. The number of valid T/P data varies for each track, some years there are very few data for 1–2 months (for example, May–July 1998 for track 112 and July–August 1993–1995 for track 187), which reduces the accuracy of the river discharge estimations at the monthly and annual scale.

4.4. Comparison between observed (in situ) and TOPEX/Poseidon-based river discharge

The calculation of daily discharge values is most successful when using data for the ground track 187 (track with the most complete data set). Comparison of T/P-derived discharge and in situ data for Salekhard is shown in Fig. 4 for the overlapping period 2000–2002, the average error (median value) is 675 m^3/s or 8%. Satellite estimates compared to in situ data give an r^2 of 0.99 (number of observations n=54). This regression gave a slope 0.99 and intercept of 265. No wonder, the maximal errors in calculating daily errors are observed during the most complicated hydrological phase—ice break-up and the beginning of spring flood. Water movement in the riverbed at this time is far from regular and thus

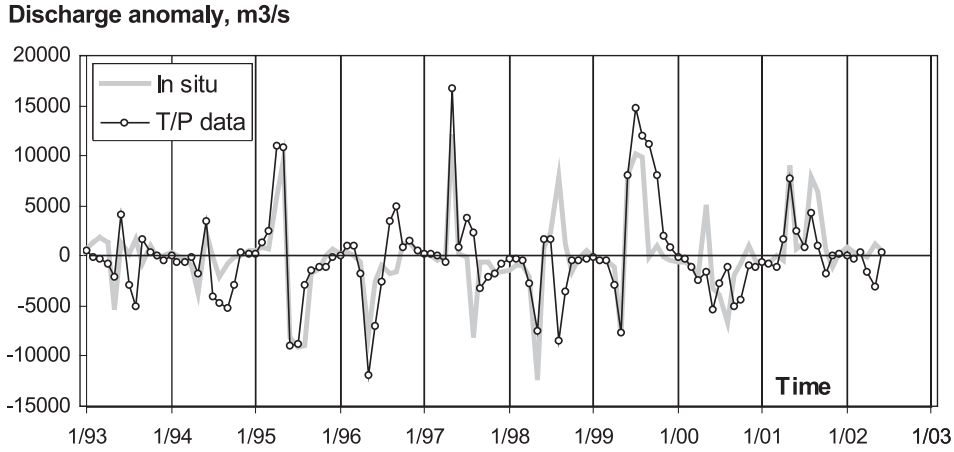

Fig. 5. Mean monthly anomalies (excluding seasonal variability) of water flow (m^3/s) at Salekhard, in situ and satellite-derived data (track 187).

calculation of Q is complicated by factors such as backwater and overbank flow. For these periods it is necessary to introduce transition coefficients. However, this requires additional information such as shape of the riverbed and valley and definition of levels at which water starts to cover the floodplain.

The errors on the computed daily discharge from T/P data are well within the range of errors acceptable for the establishment of stable multi-annual H–Q relation based on the in situ data of the river level and discharge according to the standards (Guidebook for the hydrometeorological stations and posts, 1958). These standards define acceptable errors as ±12% of discharge for the lower part of the rating curve (first 20% of the highest water level amplitude) and ±8–10% for the rest.

A comparison of monthly mean discharge values from in situ data and from T/P estimates for track 187 (see Fig. 5) shows a very good agreement. Satellite altimetry allows to calculate monthly values, which are important for climate and ecological numerical modelling, with mean (median values) absolute error of 1440 m^3/s (11% of annual discharge) and relative error of 17%. Maximal errors are observed during ice break-up and also during period of sharp decrease of water level (August–September) when overbank flow ends and water returns to the main river channel.

We also suppose that during the water depletion period in August–October there is a temporary water level rise in the region of ground track 187, which should be represented by yet another relation Q–$H_{T/P}$, but the scarcity of valid T/P data for this period does not allow to fully parameterise this process. In conditions of quasi-constant water discharge, observed during winter, errors related to the uncertainty of T/P water level estimation during ice period do not result in significant errors on the Q calculation.

A comparison of the annual discharges from the T/P water levels with the in situ data (Table 1) shows that the errors between the two estimates are about 400 m^3/s or 3% (median values) of mean annual river discharge. The large errors of annual flow estimations noted in 1995 and 1999 years are caused by the interpolation of discharge estimations when T/P data were not available. In this case, when the T/P data for ground track 187 are missing for more than five consecutive cycles (1.5 month), using the monthly discharge data calculated from T/P observations for ground track 112 increases the accuracy. We have implemented this approach for 1995, 1997 and 1999 (see Table 1), reducing the errors to 180 m^3/s or 1% of the annual value.

The comparison of monthly satellite and in situ river discharge anomalies for 1992–2001 shows a good agreement in the timing of the various stages of the hydrological regime and in the interannual variability caused by early or late spring flood (resulting in the shift of the observed maximal discharge timing: positive anomalies followed by negative ones for early flood and the inverse for late flood) (Fig. 5). The discrepancies observed in 1998 are due to missing T/P observations.

5. Conclusions

In this study, we compare in situ and satellite-derived estimations of the Ob' discharge at Salekhard and show that the T/P river level data can successfully be used for hydrological studies of seasonally ice-covered Arctic rivers. The accuracy of the Q estimation is good enough to estimate the daily discharges and the annual water flow with an average error of 8% and 1–3%, correspondingly. For the mean monthly discharges, the average errors increase up to 17%, mostly due to the scarcity of valid T/P observations during some periods and Q overestimation during the water depletion period in August–October. The introduction of new retracking algorithms for computing the river level will significantly increase the accuracy of the discharge estimates. The approach discussed in this article is still limited to rivers that are several kilometres wide because of the current satellite altimeters resolution. With a new generation of radar altimeters dedicated to continental hydrology, rivers with width on the order of 100 m could be monitored from space.

T/P-derived discharge estimates and other hydrological parameters, such as dates of the beginning and the end of spring flood, in combination with other hydrometeorological data (air temperatures, precipitation, snow cover extent and volume, etc.) will provide valuable information for studies of water budget and its variability for the whole Ob' watershed or selected parts and is the aim of future research.

Hydrologic sensitivity is one of the main control variables that determines the future response of the Arctic regions to large-scale climate changes. It is also one of the largest sources of uncertainty in predicting this response, because hydrologic sensitivity is, at the moment, poorly constrained by observations. Using the satellite altimetric

Table 1
Mean annual values of river discharge (in m^3/s) at Salekhard from in situ and satellite data, and errors (%) of estimation

Discharge (m^3/s) and associated error	1993	1994	1995	1996	1997	1998	1999	2000	2001
In situ data	13,750	13,070	12,560	12,490	13,440	12,870	15,000	12,220	15,390
Track 187	13,840	12,930	14,360	13,420	14,620	12,490	18,010	12,100	15,410
Error, %	−1	1	−14	−7	−9	3	−20	1	0
Tracks 187 and 112	13,850	12,960	13,260	13,450	13,620	12,510	15,907	12,150	15,470
Error, %	−1	1	−6	−8	−1	3	−6	1	−1

technique described in this paper for monitoring the main Arctic rivers would help constrain observations in the Arctic region. Altimeter estimates could complement in situ river discharge measurements for a global monitoring service of the environment. The contribution of spatial observations to continental hydrology is likely to develop increasingly in the near future: besides the new radar altimeters on board Jason and ENVISAT, the gravimetric mission GRACE will soon provide the water mass spatio-temporal variations at global and regional scale of 200 km, offering another validation source for the new global hydrologic models that are currently developed.

Acknowledgements

We are grateful to Dr. Robert Max Holmes from the Ecosystems Center, Marine Biological Laboratory in Woods Hole, MA, for kindly sending us the monthly Ob' River discharge data at Salekhard, and to Franck Mercier for kindly providing wet tropospheric corrections data. This work was partly supported by the AICSEX (Arctic Ice Cover Simulation Experiment) Project of the 5th EU Framework program, and the ACI Observation de la Terre from the French Ministry of Research.

References

ArcticRIMS. (2003).—A Regional, Integrated Hydrological Monitoring System for the Pan-Arctic Land Mass http://www.watsys.sr.unh.edu/arctic/RIMS/.

AVISO User Handbook. (1996). Merged TOPEX/Poseidon Products (GDR-Ms), AVI-NT-02-101-CN, Edition 3.0.

Berry, P. A. M. (2003). Global river and lake monitoring from multi-mission altimetry: capability and potential. The Abstracts of the Workshop Hydrology from Space, 29 September–1 October 2003, Toulouse, France.

Birkett, C. (1995). The contribution of TOPEX/POSEIDON to the global monitoring of climatically sensitive lakes. *Journal of Geophysical Research*, *100*, 25179–25204.

Birkett, C. (1998). The contribution of TOPEX NASA radar altimeter to the global monitoring of large rivers and wetlands. *Water Resources Research*, *34*, 1223–1239.

Bjerklie, D. M., Dingman, S. L., Vorosmarty, C. J., Bolster, C. H., & Congalton, R. G. (2003, 25 July). Evaluating the potential for measuring river discharge from space. *Journal of Hydrology*, *278*(14), 17–38.

Broecker, W. S. (1997). Thermohaline circulation, the Achilles Heel of our climate system: will man-made CO_2 upset the current balance? *Science*, *278*, 1582.

Bykov, V., & Vasiliev, A. (1973). *Hydrometry*. Leningrad, Russia: Hydrometeoizdat. 448 pp., in Russian.

de Olivera Campos, Ilce, et al. (2001). Temporal variations of river basin water from TOPEX/Poseidon satellite altimetry. Application to the Amazon basin. *Comptes Rendus de l'Académie des Sciences, Serie II, Sciences de la Terre et des planétes*, *333*, 1–11.

Guidebook for the hydrometeorological stations and postsIssue 6. (1958). *Part III,* "*Compilation and preparation of the hydrological yearbook*". Main Direction of Hydrometeorological Service of the Soviet of the Ministres of the USSR, Hydrometeorological publishing, Leningrad, 291 pp.

IPCC (Intergovernmental Panel on Climate Change). (2001). Climate Change 2001: The Scientific Basis. Contribution of Working Group to the Third Assessment Report of the PCC. In J.T. Houghton, et al. (Eds.) Cambridge Univ. Press, Cambridge.

Kouraev, A. V., Papa, F., Buharizin, P. I, Cazenave, A., Crétaux, J. -F., Dozortseva, J., et al. (2003). Ice cover variability in the Caspian and Aral seas from active and passive satellite microwave data. *Polar Research*, *22*(1), 43–50.

Kouraev, A. V., Mognard, N. M., Zakharova, A., LeToan, T., Grippa, M., & Cazenave, A. (2003). *Snow cover in the Ob' river watershed and its role in the formation of river discharge*. The Abstracts of the workshop Hydrology from Space, 29 September–1 October 2003, Toulouse, France.

Maheu, C., Cazenave, A., & Mechoso, C. R. (2003). Water level fluctuation in La Plata basin (South America) from TOPEX/Poseidon satellite altimetry. *Geophysical Research Letter*, *30*, 3.

Mercier, F. (2001). *Altimétrie spatiale sur les eaux continentales: Apport des missions TOPEX/POSEIDON et ERS-1 and 2 á l'etude des lacs*. mers intérieures et bassins fluviaux., PhD thesis. Université Paul Sabatier.

Mercier, F. (2003, April). Satellite altimetry over non-ocean areas: An improved wet tropospheric correction from meteorological models. *EGS-AGU-EUG Joint Assembly*. France: Nice.

MrSID Image Server. (2003). NASA Earth Science Application Directorate, https://www.zulu.ssc.nasa.gov/mrsid/.

Papa, F., Legresy, B., Mognard, N., Josberger, E. G., & Remy, F. (2002). Estimating terrestrial snow depth with the TOPEX/Poseidon altimeter and radiometer. *IEEE Transactions on Geoscience and Remote Sensing*, *40*, 2162–2169.

Peterson, B. J., Holmes, R. M., Mc Clelland, J. W., Vörö smarty, C. J., Lammers, R. B., Shiklomanov, A. I., et al. (2002). Increasing river discharge to the Arctic ocean. *Science*, *298*, 2171–2173.

Rahmstorf, S. (1995). Bifurcations of the Atlantic thermohaline circulation in response to changes in the hydrological cycle. *Nature*, *378*, 145–149.

R-ArcticNet. (2003). v. 2.0—A Regional, Electronic, Hydrographic Data Network For the Arctic Region, http://www.r-arcticnet.sr.unh.edu/.

Ranz, S. E., et al. (1982). Measurement and computation of streamflow: Volume 2. Computation of discharge. Water Supply Paper 2175, U.S. Geological Survey, pp. 285–631.

Russia: River basins. (1999). Ekaterinbourg, 520 pp. In Russian.

Shiklomanov, A. I., Lammers, R. B., & Vorosmarty, C. J. (2002). Widespread decline in hydrological monitoring threatens Pan-Arctic research. *EOS Transactions AGU*, *83*, 13–16.

State Water Cadaster. (1971). *Annual observations data*. Ob' river basin. (in Russian).

World Atlas of Snow and Ice Resources. Moscow, Russia: Russian Academy of Sciences.